IPPJ-AM-62

LOW ENERGY ATOMIC COLLISION RESEARCH USING HIGHLY CHARGED IONS FROM EBIS AND OTHER ION SOURCES

H. TAWARA

INSTITUTE OF PLASMA PHYSICS
NAGOYA UNIVERSITY

NAGOYA, JAPAN

IPPJ-AM-62

LOW ENERGY ATOMIC COLLISION RESEARCH USING HIGHLY CHARGED IONS FROM EBIS AND OTHER ION SOURCES#

Hiroyuki TAWARA

Institute of Plasma Physics, Nagoya University
Chikusa-ku, Nagoya 464-01, Japan

December 1988

#Invited talk given at International Symposium on Electron Beam Ion Sources and Their Applications, Brookhaven National Laboratory, Nov. 14 – 18, 1988

Abstract

In this paper we review some topics of low energy atomic physics researches involving highly charged ions produced in EBIS and other ion sources : 1) collisions with atoms, 2) collisions with electrons and 3) collisions with solids.

I. Introduction

In the past ten years, a lot of information has become available on collisions of highly charged ions with atoms and solids. Among many thrusts toward such activities, the most intense came from high temperature fusion plasma research programs in various countries. Indeed, a number of the investigations on highly charged ions have been supported by the fusion communities.

On the other hand, the timely development of very powerful ion sources capable of producing highly charged ions such as electron beam ion sources (EBIS) or electron cyclotron resonance ion sources (ECR) has contributed significantly to obtaining reliable information on various collision processes.

II. Collisions with electrons

A lot of experimental and theoretical data of ionization processes of atoms by electron impact have been accumulated[1]. However, it is quite recent that precise measurements of the cross sections for ionization of ions, in particular highly charged ions, have become possible. Some reviews on this subject are available[2].

1. Experimental techniques :

1.1 Crossed-beam method

In measurements of the cross sections for ions in collisions with electrons or ions, a series of advanced techniques such as ultra-high vacuum or precise beam controlling systems are required. The most reliable technique for determining the cross sections of excitation/recombination/ionization of ions by electrons is the ion-electron crossed beam method developed by Dolder et al.[3] and most widely used presently. In principle, this method is so-called absolute measurement and can be applied over a wide range of collision energy from meV to keV and a number of parameters have to be accurately measured . However, in some experiments serious care is necessary to avoid spurious effects such as the space potential due to electron or ion beam which changes the actual collision energy or the focusing of beams and the pressure modulation by the chopped beams. Another important parameter is the presence of the metastable state beams, which is manifested through non-zero cross sections observed even below threshold energy of the process in a number of the cases.

1.2 Trapped ion technique

Ions are trapped magnetically or electrostatically. Usually only relative cross sections can be determined through this method. In particular, only less accurate cross sections are obtained for ions with much contribution of multiple ionizations. Some models or assumptions are necessary to interpret the results.

It should be pointed that measurements based on this technique using EBIS, a kind of the ion traps, have been performed to estimate a number of ionization cross sections[4].

1.3 Plasma spectroscopy technique

Only the rate coefficients, averaged over the energy distributions, can be obtained with this method by observing particular transitions relevant to the ions (under assumptions or models on plasma conditions or plasma parameters). Though less reliable (> a factor of two at best), this is the only method for obtaining data for very high charge state ions presently.

2. Ionization processes

2.1 Single or double ionization

The ionization of atoms or ions can occur through various processes :

a) single direct (knock-out) ionization

$$e + A^{q+} \rightarrow e + A^{(q+1)+} + e$$

has been most intensively investigated and generally is believed to be dominant over multiple ionization. Indeed for light ions, this is the case.

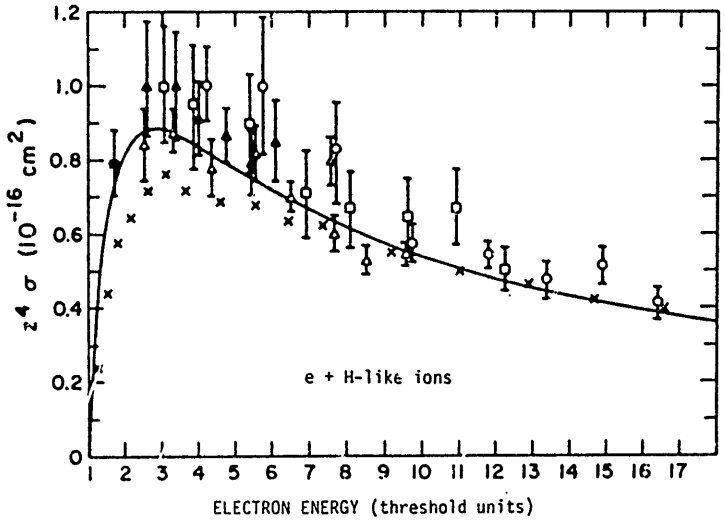

Fig.1a Scaled ionization cross sections for H-like He, C, N, O, Ne and Ar ions by electron impact. The solid curve is based on Coulomb-Born scaling for $z=128^2$. x : He, o : C, □ : N, △ : O, ▲ : Ne, * : Ar.

Even for heavy ions with hydrogen-like structure where only the direct process is possible as all the autoionization states of two electron systems are below ionization threshold, the ionization cross sections, scaled as z^4 (see Fig.1a), can be estimated with relatively good accuracy through formulas based on direct ionization mechanism (see 2.4).

Note that in very recent measurements[4a] the ionization cross section for U^{91+} ions which are determined in passing 405 MeV/amu UP^{91+} ions (which correspond to 222 keV electron velocity) through channeling directions of single crystals is found to be 3.7 b (giving the scaled cross sections z^4*s $2.8*10^{-16}$ cm^2) which is far large than the relativistic calculation of Scofield (1.5 b)[4b] and the Lotz empirical value (0.7 b)[4c] but agrees well with the relativistic K-shell ionization cross sections by Kolbenstvedt (2.98 b)[4d].

These comparisons of the cross sections indicate that reliable treatments of relativistic effects in ionization of heavy ions are necessary.

On the other hand, for many electron ions, in addition to the direct ionization processes, a number of other proceses have been found to significantly contribute to their ionization. As shown in Fig. 1b, the ionization cross sections for ions with the electron configuration of $2s^22p^n$ are mainly due to direct ionization and can be described weel with lotz empirical formula (see later), meanwhile those for ions with $3s^23p^n$ configuration show different features[4e] and are found to be significantly deviated from the Lotz formula.

b) One of them is the innershell excitation-autoionization :

$$e + A^{q+} \rightarrow e + A^{q+*}$$
$$\rightarrow e + A^{(q+1)+} + e.$$

The first process produces ions with core excitation (intermediate or compound state) which decay by the second process (autoionization) (or decay also by radiative emission that does not result in ionization. However, radiative

processes ($\cong z^4$) become dominant for high z ions). As the excitation cross sections are largest at the threshold, the cross sections for this process show sharp jumps near the threshold.

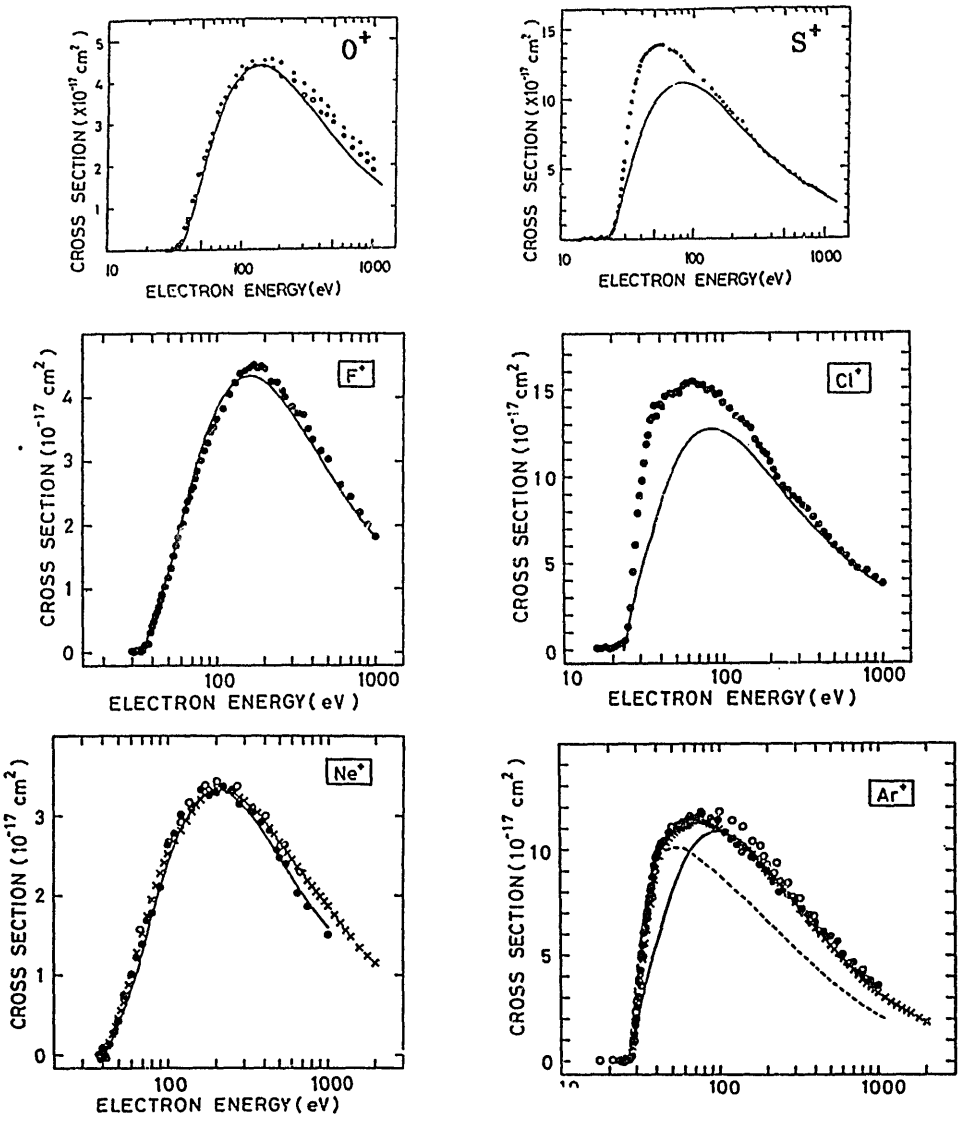

Fig. 1b Comparison of cross sections for ions with different electronic configurations[4e]. On the left are the ions with $2s^2 2p^n$ configuration (O^+, F^+, Ne^+) and on the right are those with $3s^2 3p^n$ configuration (S^+, Cl^+, Ar^+).

Related with this process, there are some other forms of the decays which result in production of higher charge ions :

b') innershell excitation-double autoionization

$$e + A^{q+} \rightarrow e + A^{q+*}$$
$$\rightarrow e + A^{(q+1)+*} + e$$
$$\rightarrow e + A^{(q+2)+} + e + e.$$

b'') innershell excitation-auto double ionization

$$e + A^{q+} \rightarrow e + A^{q+*}$$
$$\rightarrow e + A^{(q+2)+} + 2e$$

c) the resonant recombination-double autoionization is another kind of collisions with electrons :

$$e + A^{q+} \rightarrow A^{(q-1)+**}$$
$$\rightarrow A^{q+*} + e$$
$$\rightarrow A^{(q+1)+} + e + e$$

The first process, where the incident electron resonantly excites one of the innershell electrons and, losing almost all its energy, is captured into highly excited state of the ions, forms a doubly excited state, which in turn decays through two (double) successive autoionization. The cross sections are more resonant than process b).

There is another form of decays for this process :

c') resonant recombination-auto double ionization

$$e + A^{q+} \rightarrow A^{(q-1)+*}$$
$$\rightarrow A^{(q+1)+} + 2e$$

Here the first in process c) is followed by a single Auger electron emission process. In the second process, some correlation effects are expected to play a role.

d) innershell ionization-autoionization

$$e + A^{q+} \rightarrow e + A^{(q+1)+*} + e$$
$$\rightarrow e + A^{(q+2)+} + e + e$$

Here are also two decay modes possible : autoionization and Auger emission. The contribution of processes b)-d), called as "indirect" processes, become

significant with increasing the ionic charge of ions and is dominant over the direct process a) for a number of heavy ions with many electrons. Of course, it is not easy to separate the contribution from various processes.

Experiment involving many electron alkaline earth metal systems dramatically show remarkable increase of ionization cross sections. Note that for low z ions (Be^+, Mg^+) such an enhancement is not seen, meanwhile for the largest z ions (Ba^+) the enhancement is strongest. As their energy resolution was not so good, only broad peaks have been observed in these cross sections curves[5](see Fig.2). Later experiments with much better energy resolution revealed a series of peaks corresponding to excitation-autoionization processes.

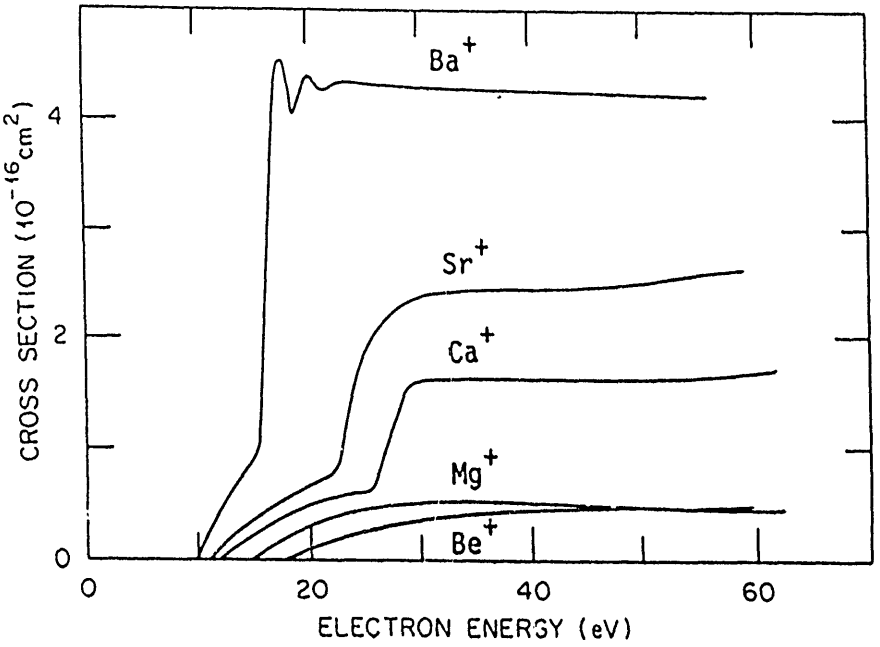

Fig.2 Cross sections for single electron ionization of Be^+, Mg^+, Ca^+, Sr^+ and Ba^+ ions by electrons[5].

For Xe^{q+}(q=2-6 ; Xe^{2+}, for example, has the electronic configuration $4d^{10}5s^25p^4$) ions, the contribution of the indirect processes increases with increasing the ionization stage and is most significant at lower energies and the observed values approach the direct ionization cross sections at highest energies. It is found that 4d-nl(nl=4f,5d,5f) excitation-autoionization can

roughly account for the observed results[6] (Xe^{6+} = $4d^{10}5s^2$) (see Fig. 3a). On the other hand, the dominant contributions of 2p-shell ionization-autoionization are observed in double ionization processes for Ar ions[2](see Fig. 3b). Note that, though double ionization cross sections below 2p ionization threshold decrease for higher ionization states, 2p ionization cross sections tend increase with increasing the ion charge state while their 2p ionization energies increase.

However, there are some examples which can not be explained only through such "indirect processes". Indeed there is a serious discrepancy in ionization of, for example, Fe^{15+} ions which is expected to have intense resonant excitation-double autoionization at around 760 eV[7] (Fig. 4). On the other hand, very recently, the contribution of resonant recombination-autoionization processes

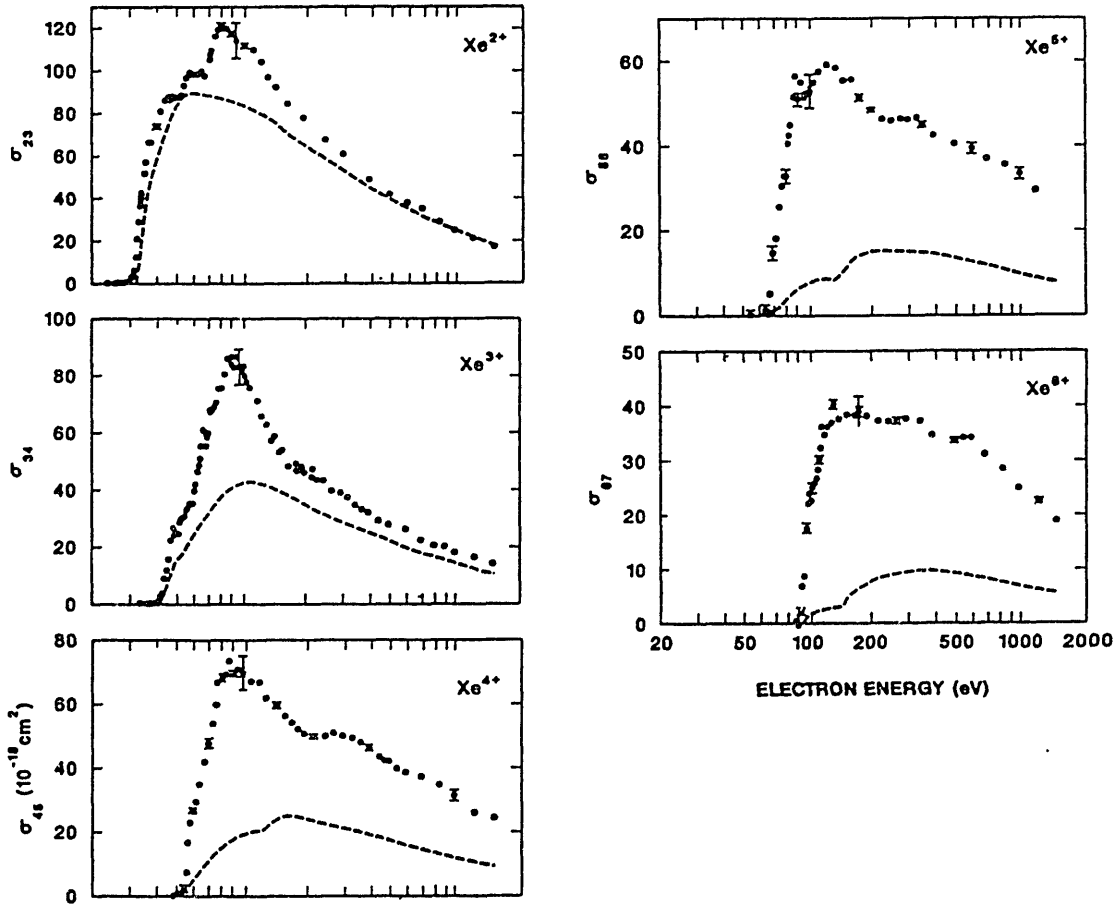

Fig. 3a Cross sections for single electron ionization of Xe^{q+}(q=2-6) ions by electrons[6].

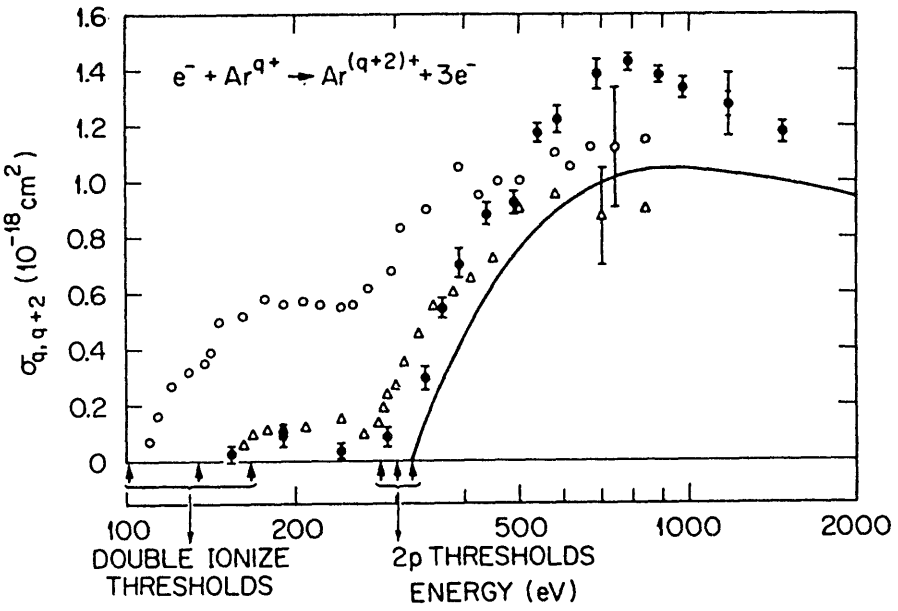

Fig. 3b Cross sections for double ionization of Ar^{q+} (q=2,3,4) ions by electrons. The solid curve represents the distorted-wave calculation for direct 2p ionization of Ar^{4+} . o : q=2, △: q=3, ● : q=4.

has been confirmed for C^{3+} ions, though it is weak (≅1% of direct ionization)[8]. We need our extensive studies of ionization of various ions with different electronic configurations.

2.2 Multiple ionization

Multiple ionization is generally weak, relative to single ionization. It should be noted that deeper innershell ionization (excitation) processes, followed by successive (cascade) autoionization or Auger electron emissions, contribute dominantly to multiply-charged ion production. In fact, the cross sections for L- and K-shell ionization of Ar atoms by electrons become comparable to those for Ar^{2+} and Ar^{5+} ion production from Ar atoms[9] (see Fig.5). Systematic measurements of cross sections have to be made for various ions.

2.3 Threshold behaviors

The cross sections for ionization for ions are known to be zero at the

threshold (significantly different from excitation processes) and, then, increase with increasing the impact electron energy E just above threshold. There are slight differences in their behaviors among neutrals and ions in ionization by electrons : for neutrals, the inter-electron repulsion is important, meanwhile for ions the electron-ion attractive interaction plays a role.

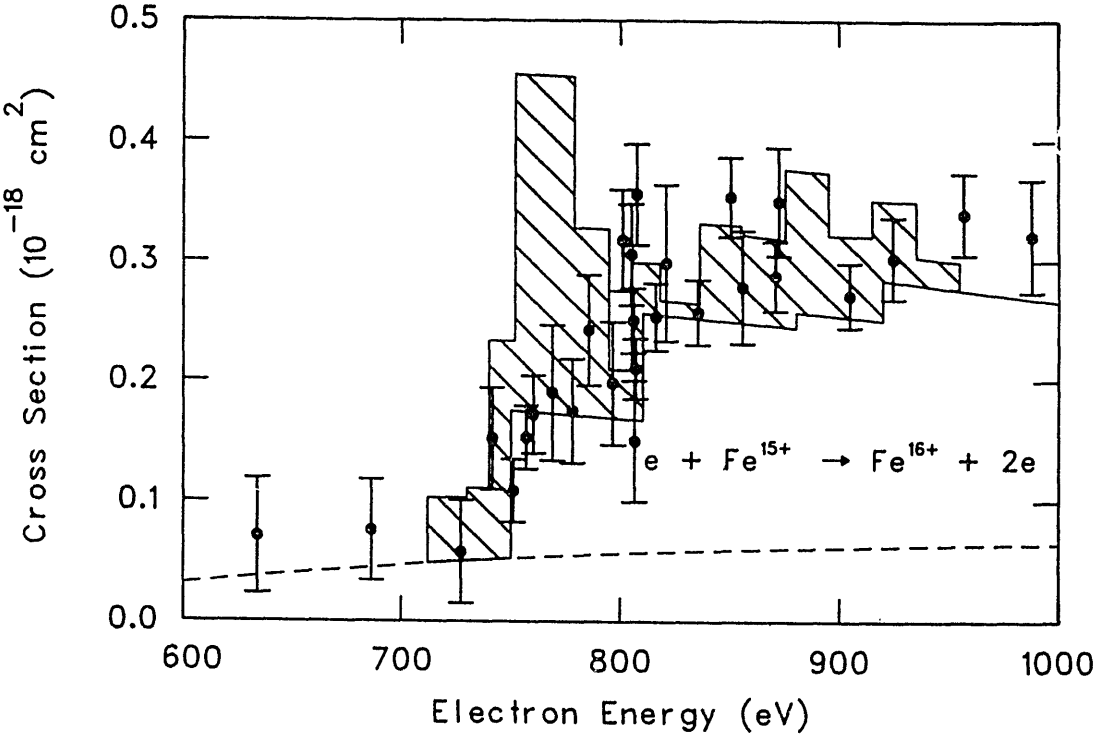

Fig.4 Cross sections for single electron ionization of Fe^{15+} ions by electrons[7]. The dotted and solid lines represent the direct and excitation-autoionization contributions, respectively. The shaded part is due to the resonant-excitation double autoionization. The experimental data are shown with the solid circles with error bars[7].

Very roughly speaking the following constants for their power are proposed[10] :

$\sigma \cong E^a$ ($a_1 \cong 1$ for single ionization : $a_n \cong n$ for n-times ionization).

However, there exist no systematic studies on the threshold behaviors in ionization of ions, in particular their multiple ionization processes of highly charged ions. Such experiments often encounter the presence of the metastable

ions in parent beams. Very small fractions of such beams excludes the possibilities in working at the threshold region where the cross sections should be small.

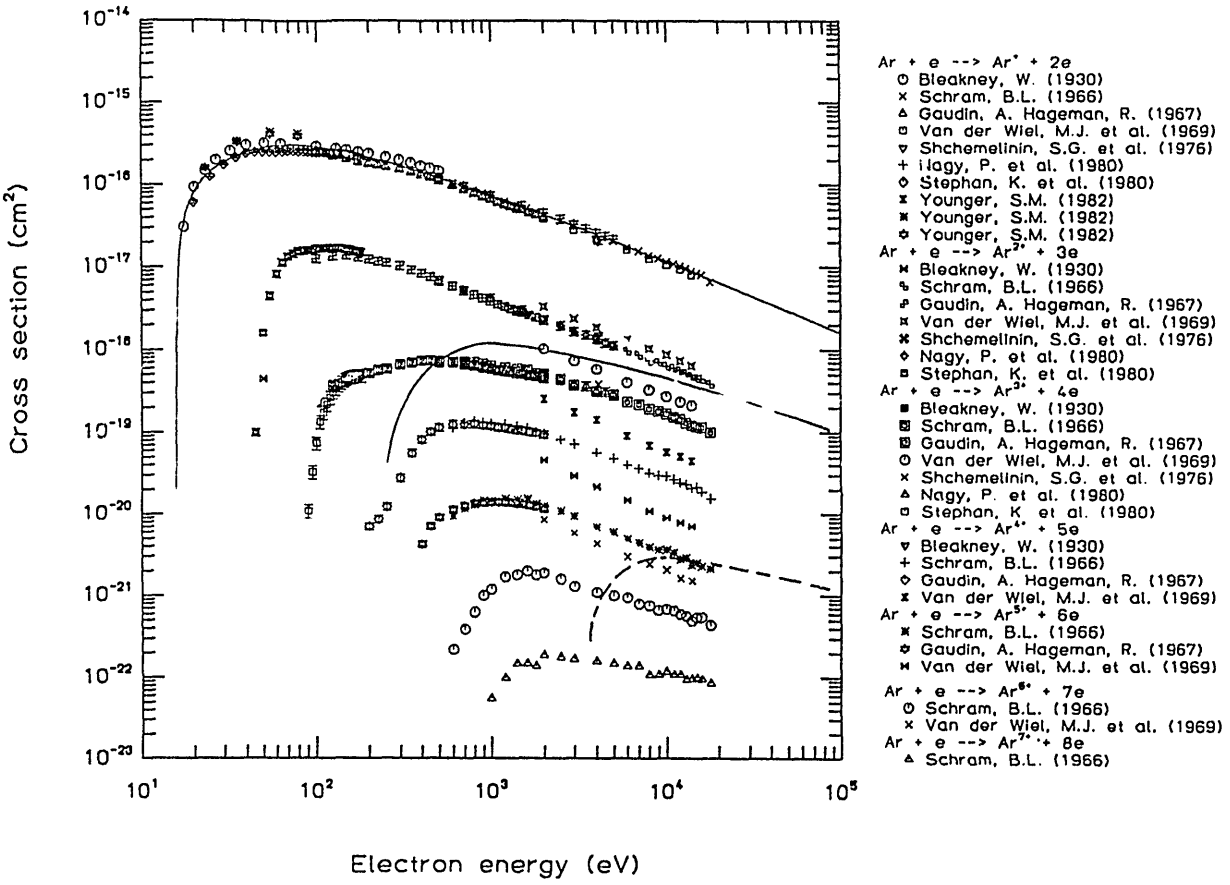

Fig.5 Comparison of cross sections for (i=1-7) multiple ionization and (L- and K-) innershell ionization of Ar atoms[9].

2.4 Empirical formulas for ionization cross sections

Lotz formulas, based upon Born approximation for direct ionization, are most widely used[11]. If plotted as $\sigma * I_j^2$ versus E/I_j (σ is the ionization cross sections : I_j is ionization potential of electrons in the j-th shell and E is electron impact energy), all data must fall on a single line, as seen in Fig.1 above. For H-like ions, the ionization cross sections scale as z^4. It must be noted that this formula is valid only for direct ionization. There are many

proposed formulas which have their limited validity. However, no simple scaling formulas which include those for indirect processes are available.

3. Excitation processes

3.1 Threshold and resonance

Excitation of ions by electron impact has its feature whose cross sections become maximum at the thresholds, in contrast with that of neutral atoms by electron impact[2,12]. Another important feature near the threshold region is the occurrence of a series of resonances where the cross sections show their significant jumps. Although their widths are narrow, their contribution to total excitation cross sections is significant. The resonances are the consequence of the formation of some intermediate (compound doubly excited) autoionizing states during the incident electron-ion collisions which decay through emission of electrons. These resonance behaviors and contribution to the mean cross sections have to be calculated carefully using the reliable theories or approximations. For H-like ions, the resonance contribution to the 1s->2s and 1s->2p excitation (due to $3s^2$, $3p^2$ and $3d^2$ autoionizing states) are estimated to be 20 and 10 %, respectively, with less contribution to the excitation to higher n-states[13].

On the other hand, at higher energies reliable excitation cross sections can be estimated using some asymptotic behaviors. For example, some empirical formulas such as Gaunt-factor formula could sometimes provide quite reasonable estimation of the excitation cross sections[2].

3.2 Experiments and data

As mentioned above, the ion-electron crossed-beam technique is the most reliable method for determining the excitation cross sections since the first experiment has been performed by Dance et al.[14] in 1966 through observing photons with particular energies. However, the obtained cross sections are generally less accurate and their uncertainties are estimated to be at best 15-

20 %, with the most serious errors being due to absolute calibration of photon detection efficiencies (10-15 %), which should be compared with those of ionization (≅2%). Up to now, most of the experimental studies have been concentrated on relatively low charge ions because of the limited availabilities of ions and N^{4+} ions is the highest in ionic charge which has been investigated[15] (see Fig. 6a).

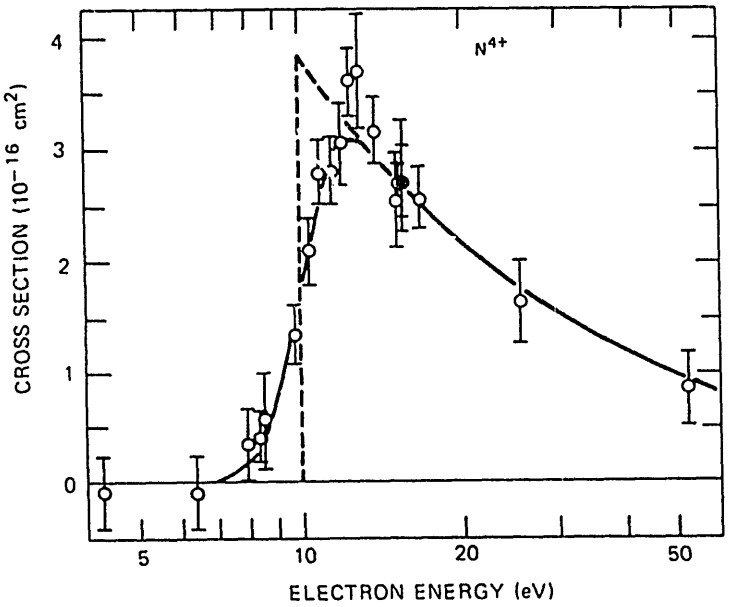

Fig. 6a Comparison of absolute 2s->2p excitation cross sections for N^{4+} ions by electrons. The dashed and solid lines represent the close coupling calculation without and with the experimental electron energy distribution, respectively[15].

A unique technique has recently been developed to determine electron impact excitation of highly charged ions through X-ray spectroscopy :
L X-rays from the highest charge state ions ever studied, Ba^{46+}, originated from electron impact excitation, have been observed in electron beam ion trap(EBIT) and the excitation cross sections at 5.69 and 8.2 keV electrons have been determined.[16]

The excitation cross sections can also be estimated through observation of distinct structures in the ionization cross section curves, as already

discussed before. In fact, this technique could be an alternate to know the cross sections of excitation of highly charged ions, though the accuracy may not be so good as those for total ionization (see Fig. 6b).

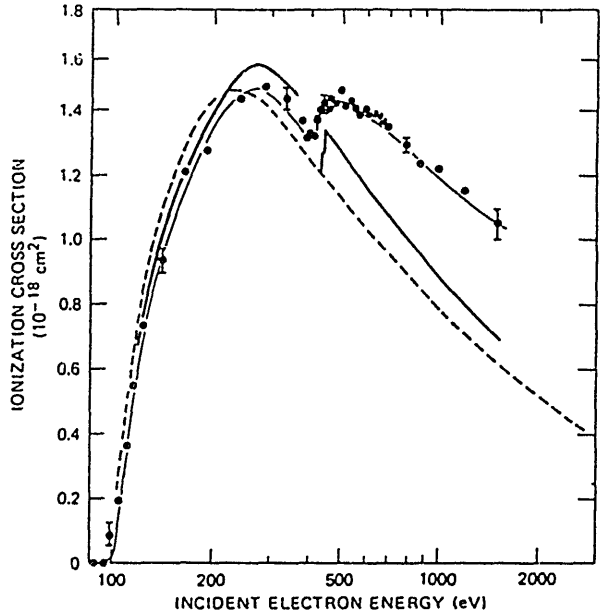

Fig.6b Excitation cross sections seen in total ionization cross sections. The solid line below 350 eV is the Coulomb-Born direct ionization, the dotted line is the scaled Coulomb-Born direct ionization and the solid line above 415 eV is the cross section for $1s^2 2s \rightarrow 1s2s2l$ excitation.[2]

To get more insight in excitation of ions by electrons, angular distributions (up to 20°) of the ns->np excitation cross sections, for example of Cd^+ or Zn^+, have been determined through observing the energy loss spectrum of scattered electrons, instead of photon detection, based on the cross-beam technique and found to be in agreement with the close-coupling calculations[17].

Up to now very few direct observations have been reported of resonances in the excitation of ions by electron impact. Experimental confirmation or investigations of the calculations for resonances in excitation of highly charged ions should be pursued systematically.

4. Dielectronic recombination(DR)

$$e + A^{q+} \rightarrow A^{(q-1)+**}$$

$$\rightarrow A^{(q-1)+**} + h\nu$$

This is another form of decays of the intermediate doubly excited states formed through recombination of electron with target ion and thus competing with autoionization processes : such states, instead of emitting electrons, decay through emitting photon (radiative decay). This is also the exact inverse process of photo-innershell excitation process followed by autoionization. Therefore, the cross sections for DR can be obtained through the following relation[18] :

$$\sigma(DR)=\sigma_c*[A_r/(A_r+A_a)]$$

where A_r and A_a are the radiative and autoionization rates, respectively.
In order to investigate DR experimentally, the coincidence between photon (hv) and product ion with one-less ionic charge ($A^{(q-1)+}$) or some resonance structures in the cross section curves or their combination is often used. However, there are serious difficulties : the product $A^{(q-1)+}$ ion has an electron in high Rydberg state which is easily influenced by their environments such as field ionization, field mixing, collisional ionization, resulting the significant loss of the product. In fact, in one of the first electron-ion crossed beam experiments of DR on Mg^+ ions[19] (see Fig.7a) :

$$e + Mg^+(3s) \rightarrow Mg^{**}(3p,nl) \rightarrow Mg^*(3s,nl) + h\nu,$$

the observed result is found to be too large, compared with theoretical calculation. This discrepancies, however, can be removed by taking into account the field ionization and mixing correctly. In other well-collimated MeV ion-high density electron merging method, such environments are also found to influence the observations.
For DR of very high charge ions, a different technique is used : 10- 100 MeV ions collides with atoms where electrons can be assumed to be quasi-free. The coincidence rates between X-ray and product ion show broad resonance-like behaviors which correspond to DR with an electron of the energy distribution

with Compton profile, instead of a free electron. As expected, however, the detailed structures of DR can not be resolved but only their gross cross sections are known with this method.

Another interesting method is the use of EBIS or EBIT itself. Directly looking into EBIS and observing X-rays as a function of the confining electron energy, DR of Ar ions has been investigated. Their cross sections are estimated to be of the order of 10^{-20} cm^2, roughly agreeing with theoretical prediction for Ar^{14+} KLL DR. However, the electron energy spread (≅15 eV mainly due to the space charge potential of the confining electrons) is too large to look at the detailed structures of DR in Ar ions[20] (see fig.7b).

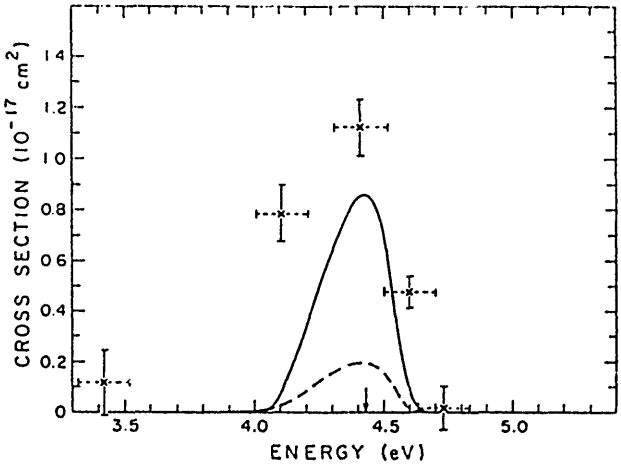

Fig.7a DR cross sections for e + Mg^+ collisions. The solid and dotted lines represent the calculations for all n and for $n \leq 64$, respectively.[18]

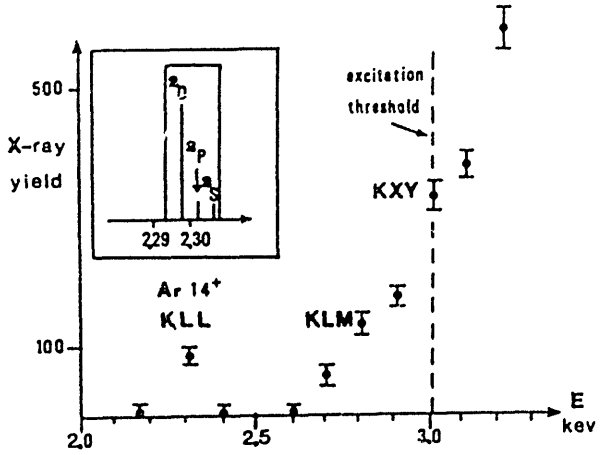

Fig.7b Ar-K-x-ray yields as a function of electron energy in EBIS[20].

References to II

1. H.Tawara & T.Kato, At. Data and Nucl. Data Tables 36 (1987) 167 ; K.L.Bell, H.B.Gilbody, J.G.Hughes, A.E.Kingston & F.J.Smith, J. Phys. Chem. Ref. Data 12 (1983) 891
2. D.H.Crandall, Atomic Physics of Highly Ionized Atoms (ed. R.Marrus, Plenum, 1982) p.399 ; R.A.Phaneuf, Atomic Processes in Electron-Ion and Ion-Ion Collisions (ed. F.Brouillard, Plenum Press, 1986) p.117
3. K.T.Dolder, M.F.A.Harrison & P.C.Thonemann, Proc. Roy. Soc. A 26 (1961) 367
4. E.D.Donets & V.P.Ovsyannikov, Sov. Phys.-JETP 53 (1981) 466

4a. N.Claytor, B.Feinberg, H.Gould, C.E.Bemis, J.Gomez del Campo, C.A.Ludemsann and C.R.Vane, Phys. Rev. Letters 61 (1988) 2081

4b. J.H.Scofield, Phys. Rev. A 18 (1978) 963

4c. W.Lots, Z. Phys. 216 (1968) 241

4d. H.Kolbenstvedt, J. Appl. Phys. 46 (1975) 2771

4e. I.Yamada, A.Danjo, T.Hirayama, A.Matsumoto, S.Ohtani, H.Suzuki, H.Tawara, T.Takayanagi, K.Wakiya and M.Yoshino, J. Phys. Soc. Japan 57 (1988) 2699 ; J. Phys. Soc. Japan (submitted)

5. B.Peart & K.Dolder, J. Phys. B 8 (1975) 56 ; R.A.Falk and G.H.Dunn, Phys. Rev. A 27 (1983) 754
6. D.C.Griffin, C.Bottcher, M.S.Pindzola, S.M.Younger, D.C.Gregory & D.H.Crandall, Phys. Rev. A 29 (1984) 1729
7. D.C.Gregory, L.J.Wang, F.W.Meyer & K.Rinn, Phys. Rev. A 35 (1987) 3256
8. A.Muller, G.Hoffmann, K.Tinchert & E.Salzborn, Phys. Rev. Letters 61 (1988) 1352
9. H.Tawara, private communication (based upon AMDIS data base, IPP, Nagoya Univ.)
10. A.R.P.Rau, Electronic and Atomic Collisions (North-Holland, 1984) p.711
11. W.Lotz, Z. Phys. 216 (1968) 241 ; T.Kato, IPPJ-AM-2 (Institute of Plasma

Physics, Nagoya Univ., 1977) ; M.S.Pindzola, D.C.Griffin, C.Bottcher, S.M.Younger & H.T.Hunter, Nucl. Fusion Suppl.(1987) 21 ; M.Arnaud & R.Rothenflug, Astron. Astrophys. Suppl. Ser. 60 (1985) 425 ; A.Burgess & M.C.Chidichimo, Mon. Not. R. astrophys. Soc. 203 (1983) 1269 ; L.A.Vainshtein & V.P.Shevelko, Opt. Spectrosc.(USSR) 63 (1987) 11

12. V.A.Bazylev & M.I.Chibisov, Sov. Phys.-Usp. 24 (1981) 278 ; Y.Itikawa, Phys. Rep. 143 (1986) 69 ; J.W.Gallagher & A.K.Pradhan, JILA (Univrsity of Colorado) report no.30 (1985)
13. M.A.Hayes & M.J.Seaton, J. Phys. B 11 (1978) 79
14. D.F.Dance, M.F.A.Harrrison & A.C.H.Smith, Proc. Roy. Soc. A 290 (1966) 73
15. D.C.Gregory, G.H.Dunn, R.A.Phaneuf & D.H.Crandall, Phys. Rev. A 20 (1979) 410
16. R.E.Marrs, M.A.Levine, D.A.Knapp & J.R.Henderson, Phys. Rev. Letters 60 (1988) 1715
17. A.Chutjian, Phys. Rev. A 29 (1984) 64
18. G.H.Dunn, Atomic Proceses in Electron-Ion and Ion-Ion Collisions (Plenum, 1986) p.93 ; Y.Hahn & K.J.LaGattuta, Phys. Rep. 166 (1988) 195
19. D.S.Belic, G.H.Dunn, T.J.Morgan, D.W.Mueller & C.Timmer, Phys. Rev. Letters 50 (1983) 339
20. J.P.Briand, P.Charles, J.Arianer, H.Laurent, C.Goldstein, J.Dubau, M.Loulergue & F.Bely-Dubau, Phys. Rev. Letters 52 (1984) 617

III. Collisions with atoms at low velocities

Generally we can write down our collision processes between highly charged ion A^{q+} and neutral atom B as follows :

$$A^{q+} + B \rightarrow A^{r+}(M) + B^{i+}(N) + (r + i - q)*e + \Delta E$$

M, N : quantum states (n,l,m) of projectile and target atom.

The most important parameters in such electron transfer processes are 1) collision velocity, 2) projectile charge, 3) electron binding energy of target atoms and 4) the number of electrons involved.

In order to get information of collision processes, we have to measure some of the followings : 1) charge-changed projectiles A^{r+}, 2) recoil ions B^{i+}, 3) coincidence between A^{r+} and B^{i+}, 4) translational energy to determine ΔE, 5) photons emitted from either $A^{r+}(M)$ or $B^{i+}(N)$ or both, 6) electrons.

At the energy range of our slow collisions ($\cong$ ev/amu-keV/amu), the dominant collision process is capture of electrons into projectile ions, but ionization process of projectile ions is usually of minor importance. In such electron capture processes, electrons are usually captured into excited states of projectile ions which, in turn after emitting photons or electrons, get relaxed. Many of the observed features can be explained with the assumption that quasi-molecules are formed during such slow collisions (see Fig. 1a).

1. Theoretical aspects

A number of theories have been developed to treat electron transfer processes at low energies. Some nice reviews are available[1].

Very qualitatively, the electronic (n,l,m) states of projectile ions after electron capture process can be understood as follows :

a) for bare ion collisions, the l-states are degenerate but their l-distributions should be influenced through Stark mixing among projectile sublevels by the electric field of target ions.

b) for partially ionized ions, this l-degeneracy is lifted and there are a

number of crossings between the entrance channel and the outgoing (n,l) sublevels (see Fig. 1a).

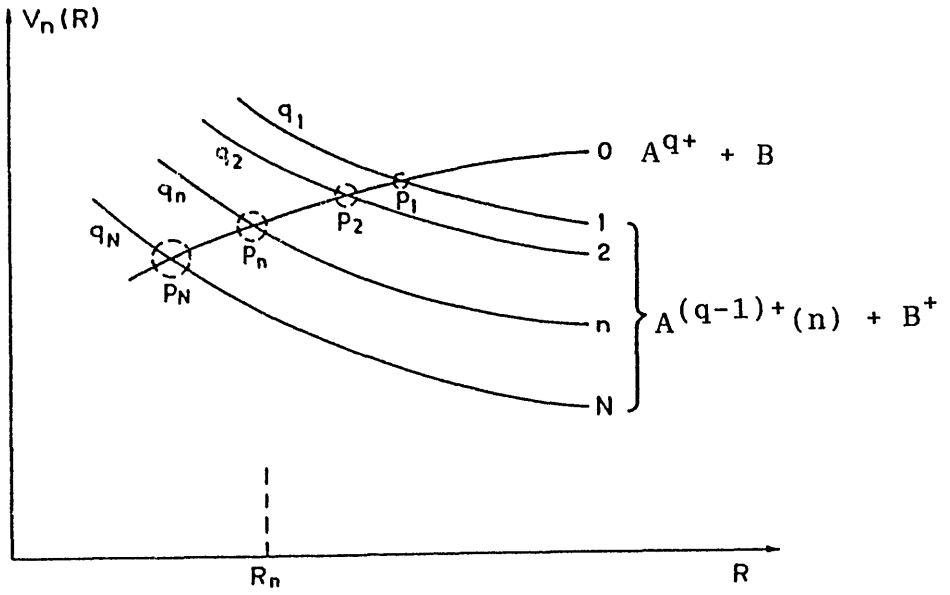

Fig.1a The potential energy curves for one-electron transfer A^{q+} + B -> $A^{(q-1)+*}$ + B^+ collisions. Note that there are a number of crossings between the incident channel A^{q+} + B and the outgoing channels $A^{(q-1)+}$ + B^+ at different positions.

c) the primary mechanism is coupling of the entrance channel with a single particular (n,l) level. However, the Stark interaction between this (n,l) level and other l-levels on the way out may change the initial (n,l) distribution (for lower l-levels, the interaction of active electron with ion core > Stark effect).

Among theories and models, the classical over-barrier model is most convenient for understanding and explaining the expected and observed phenomena[2] (see Fig. 1b). Based upon this model, total cross sections and the electron-capturing n-state (the most probable quantum state) can be estimated roughly. The Landau-Zener (LZ) model is also quite useful for more qualitative as well as

quantitative (though not accurate) understanding of this process (here the radial coupling is assumed to be dominant). The LZ model is easily extended for multi-channel crossings[3] by taking into account transitions at a series of crossings(see Fig. 1c). Further modification of LZ formula can be used to explain the l-distributions[4].

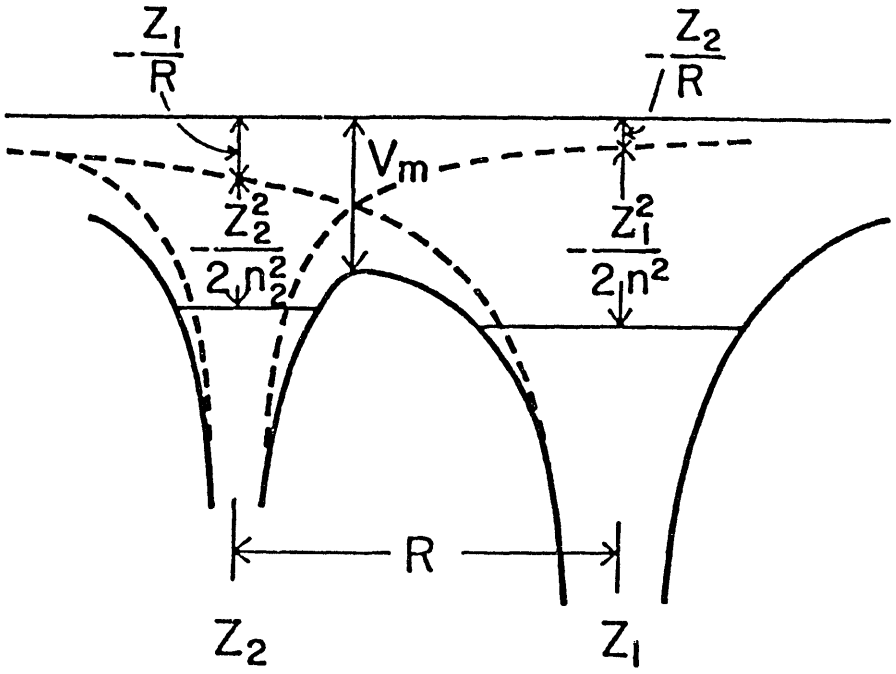

Fig. 1b Classical over-barrier model. With projectile ion z_1 approaching neutral atom z_2, the potential energy curves of both collision partners are varied. If the Coulomb barrier V_m is overcome by this proximity and a proper vacant level is available in projectile ion, an electron of target can jump into that level.

2. Total electron transfer cross sections

Total cross sections do not strongly depend on the collision energy of our interest[5], except for very light ions (see Fig.2). This is because there are a number of curve-crossings at proper region of impact parameters (collision or reaction window[4]) for highly charged ions.

Based upon a number of available data[6], a number of useful empirical formulas[1]

to estimate total cross sections for various ion-atom combinations are proposed[5]. One of the most convenient scaling formulas for total electron capture cross sections is given :

$$\sigma_{q,q-k} = A*q^{a}*I^{b} \qquad (k=1\text{-}4) \qquad (1)$$

where I is the ionization potential (eV) of target atom, q the ionic charge of incident ion, A, a and b constants depending on k, the number of electrons captured[5]. These parameters for k=1-4 are given in Table 1.

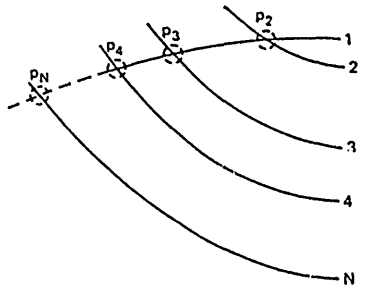

$$P_{1j} = (p_2 p_3 \cdots p_j)(1-p_j)\{1+(p_{j+1}p_{j+2}\cdots p_N)^2+(1-p_{j+1})^2+[p_{j+1}(1-p_{j+2})]^2+[p_{j+1}p_{j+2}(1-p_{j+3})]^2$$
$$+\cdots+[p_{j+1}p_{j+2}\cdots p_{N-1}(1-p_N)]^2\},\quad j<N-1,$$
$$= (p_2 p_3 \cdots p_{N-1})(1-p_{N-1})[1+P_N^2+(1-P_N)^2],\quad j=N-1,$$
$$= 2p_2 p_3 \cdots p_N(1-p_N),\quad j=N.$$

Fig. 1c Multichannel Landau-Zener model with N-1 crossings.

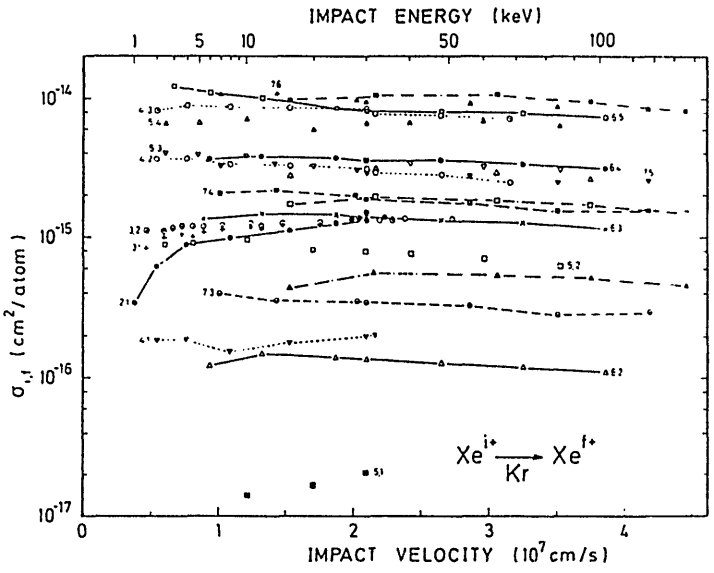

Fig.2 Energy dependence of total electron capture cross sections for Xe^{i+} + Kr -> Xe^{f+} collisions[5].

Table 1 Least square fit parameters of equation (1)

to calculate cross sections

k	1	2	3	4
A (cm^2)	$1.43*10^{-12}$	$1.08*10^{-12}$	$5.50*10^{-14}$	$3.57*10^{-16}$
a	1.17	0.71	2.10	4.20
b	-2.76	-2.80	-2.89	-3.03

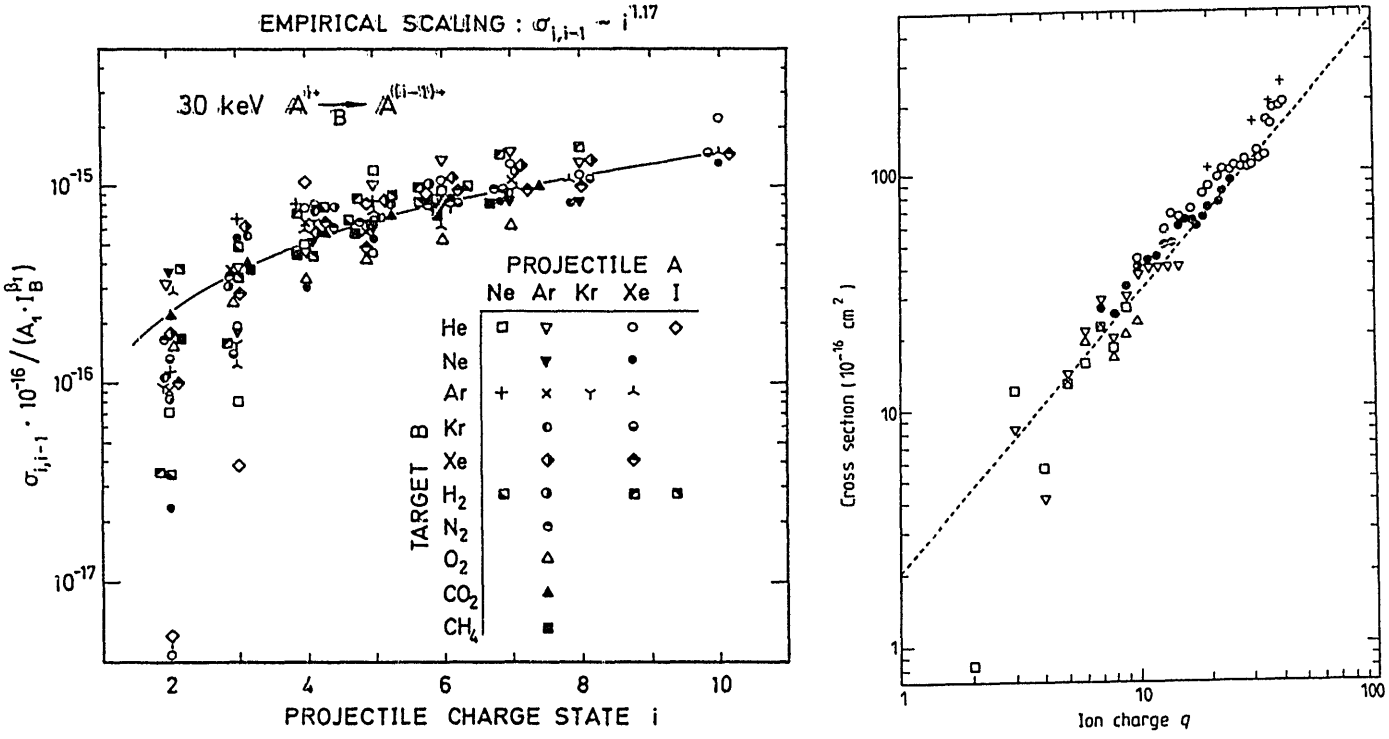

Fig.3a Scaled total cross section curve in comparison with experimental data. a) low q ions[5] ; b) high q ions (Kr, Xe and I for He gas)[7].

As an example of fitting these data, in Fig. 3a is shown a comparison between a fitting curve and experimental data for single electron capture processes in various ion-target combinations. Note that there are serious scatterings of data at lower charge states, compared with the fitted curve. In fact, for low q ions, sharp resonance-like variations of the cross sections are observed. This oscillation, understood quantitatively from quantal theory as well as the

classical over-barrier model, is due to resonance of the energy levels between projectile and target atom because there are available only a limited number of the energy levels for light elements[6a] (see Fig. 3b). Data up to q = 42 from He target are found to follow well with this empirical formula[7] (see Fig. 3a). Here we should note, according to recent calculation by Gargaud and McCarroll[7a] that even total cross sections can not be scaled anymore at the energy less than 0.1 keV/amu because of strong core electron effects, though not confirmed experimentally yet (see Fig. 3c).

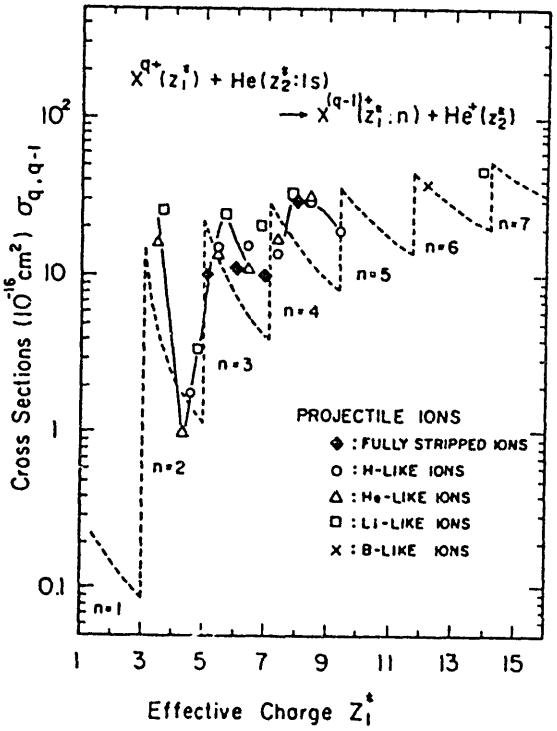

Fig.3b Oscillation of electron capture cross sections at low q ions with He[6a]. Note significant oscillations of cross sections at low ionic charge.

For highly charged projectiles, in particular in collisions with multi-electron targets, not only single electron transfer process but also multiple electron transfer processes play an important role. In some cases (such as C^{4+} + He system), two-electron transfer has been observed to be dominant over single-electron transfer process at low energies[8]. In multiple electron transfer

processes, electron transfer into projectile from target atom simultaneously accompanied with target ionization (transfer ionization) can be one of the important processes in production of multiply charged recoil ions. It is found that in triple electron capture from neutral Xe target atoms by Xe^{8+} ions, the most intense recoil Xe ions have the charge 5+ which means two more electrons are lost from target through autoionization (see Fig.4).

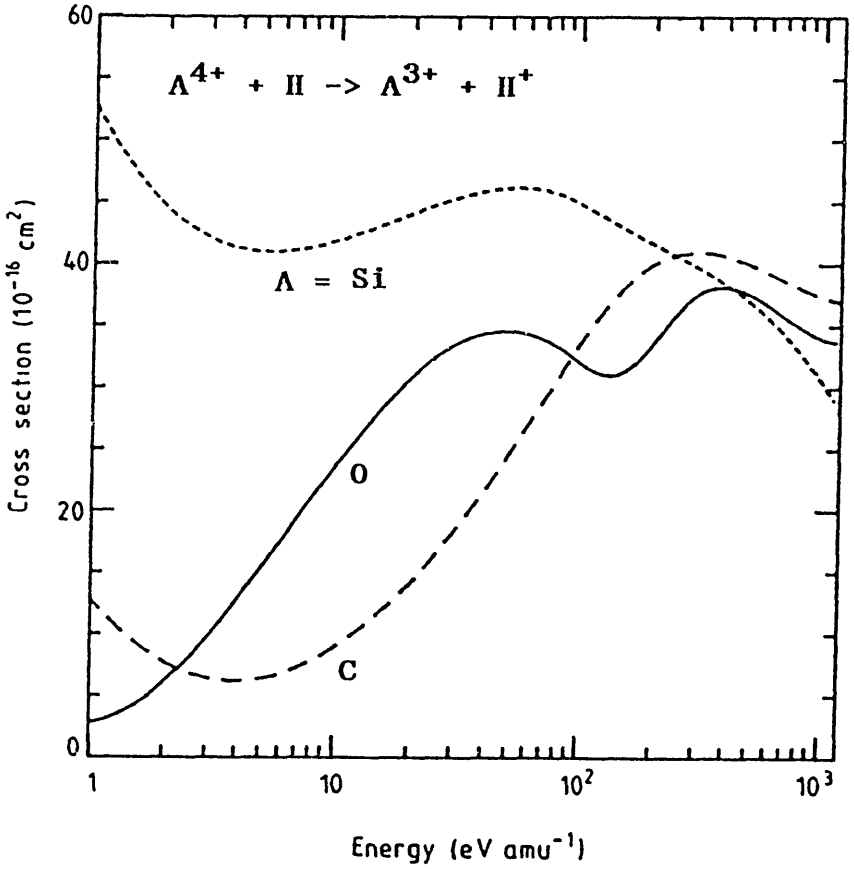

Fig. 3c Total single electron capture cross sections for ions with the ionic charge 4 in collisions with atomic hydrogen[7a] at very low energies.

It should be pointed out that total cross sections for very high charge state ions are still limited in particular for many electron targets including molecules and also that total cross sections of such highly charged ions at very low energies of meV/amu - 1 eV/amu are particularly important in applications to astrophysics. Yet very few work has been reported[10].

It should be noted that, though important in some fields, electron transfer between highly charged ions has been rarely investigated, except for singly or doubly charged ions, to compare theoretical calculations[10a].

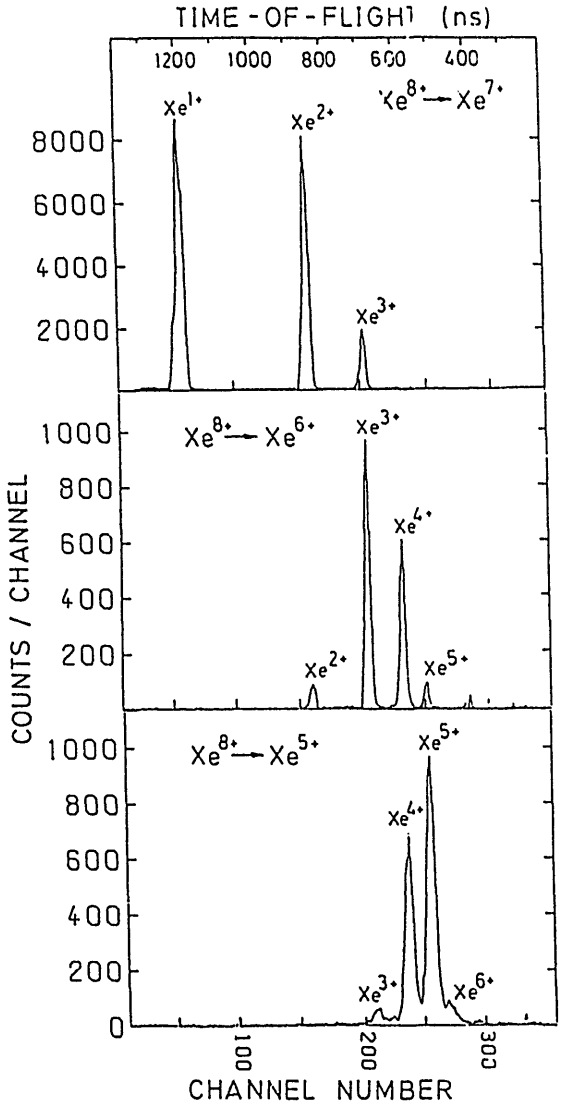

Fig.4 Correlation of projectile ions and secondary (recoil) ions produced in 80 keV Xe^{8+} + Xe collisions[9].

3. (n,l,m) partial cross sections

3.1 n-distributions

Through a series of observation of translational energy(-gain) spectroscopy, some scaling laws for estimating the most probable n-state have been introduced

for light atoms such as He^7 (see Fig.5) :

$$n_0 = 0.76*q^{0.818}$$

which can be compared with the classical over-barrier model :

$$n_0 = 1.414*(q/z_2)^{0.75}$$

where z_2 is the effective charge of target atom.

Again we should stress that no simple scaling laws can be found at low energies to estimate n_0 (see Fig. 6).

For many-electron targets, multi-electron capture becomes comparable with single electron capture and both the resultant projectile and target may be in their excited states, both forming possibly multiply excited states and being autoionized. **Systematic investigations on the correlated (M,N) states have to be performed.**

3.2 (n,l)-distributions

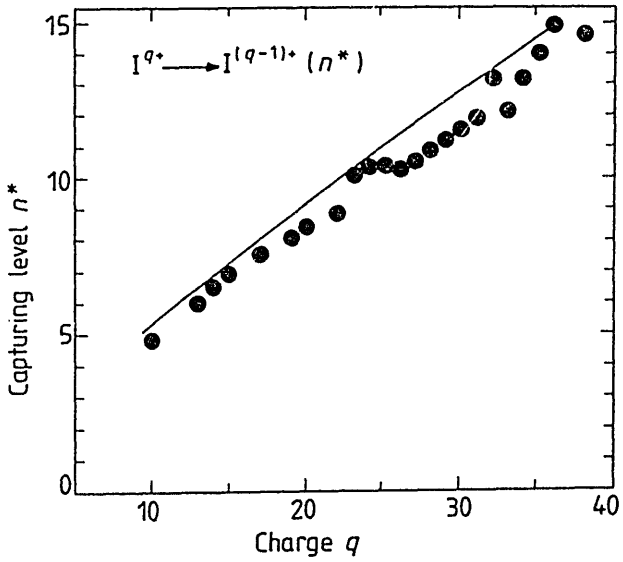

Fig.5 The most probable quantum n-state of highly charged I^{q+} (q=10-38) ions into which an electron is captured from He atoms[7]. The solid line is due to the classical over-barrier model.

The l-distributions should be influenced through Stark mixing among projectile sublevels by the electric field of residual target ions. For partially ionized

ions (l-sublevels are not degenerate anymore but separate), intrashell Stark mixing among l-subshells due to target ion becomes diminished and the final (l,m) distributions are determined by the interaction of electrons captured into the outer-shell with the core electrons in projectile (core effect). Indeed significant core effect is predicted in charge transfer of highly charged ions (see Fig.6). At low energies, as mentioned already, even total cross sections are strongly dependent upon projectile ions themselves even if they have the same ionic charge[11] (see Fig. 3c).

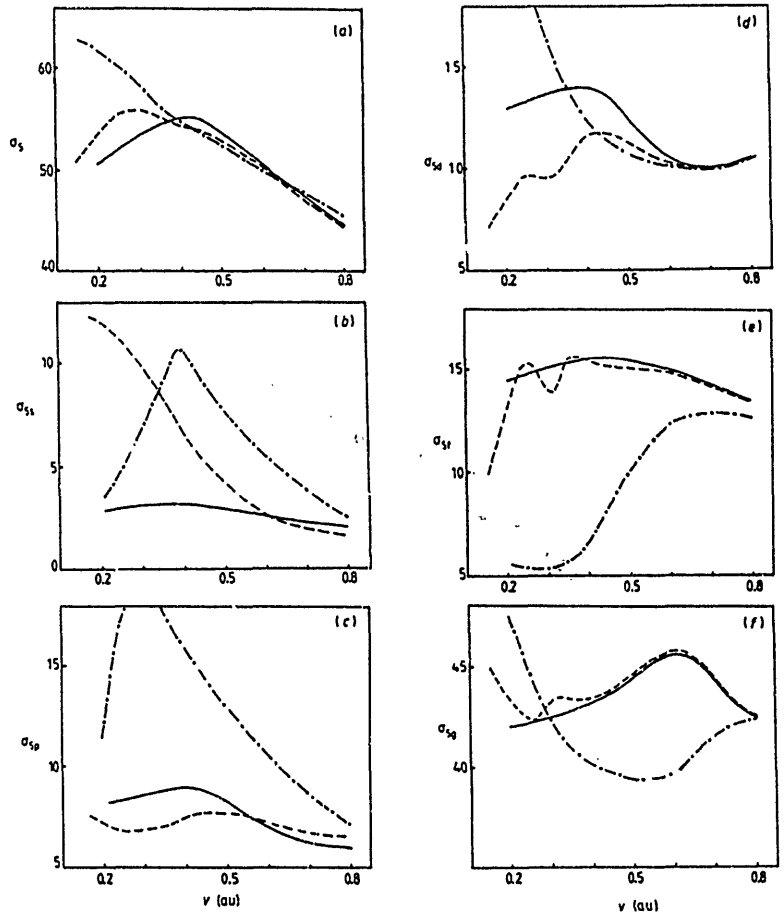

Fig.6 Partial cross sections for electron capture into 5l states of A^{7+} ions in collisions with atomic hydrogens as a function of collision velocity [A = O(solid line), Ne(dotted line), Ar(dash-dotted line)]. a) total for n=5, b) 5s state, c) 5p state, d) 5d state, e) 5f state, f) 5g state.

Thus, there seems almost no way to infer or find any empirical formula to estimate the partial (n,l) cross sections at very low energies. Detailed studies for individual cases should be performed to get reliable information on (n,l)-distributions. On the other hand, only a limited experimental information on (n,l) distributions is available. The l-distributions are found to be strongly dependent on the velocity[11,12]. The observed results confirm most theoretical calculations only for dominant channels in (n,l) distributions, meanwhile those for less dominant channels are different from each other where theoretical calculations become difficult[13](see Fig.7a).

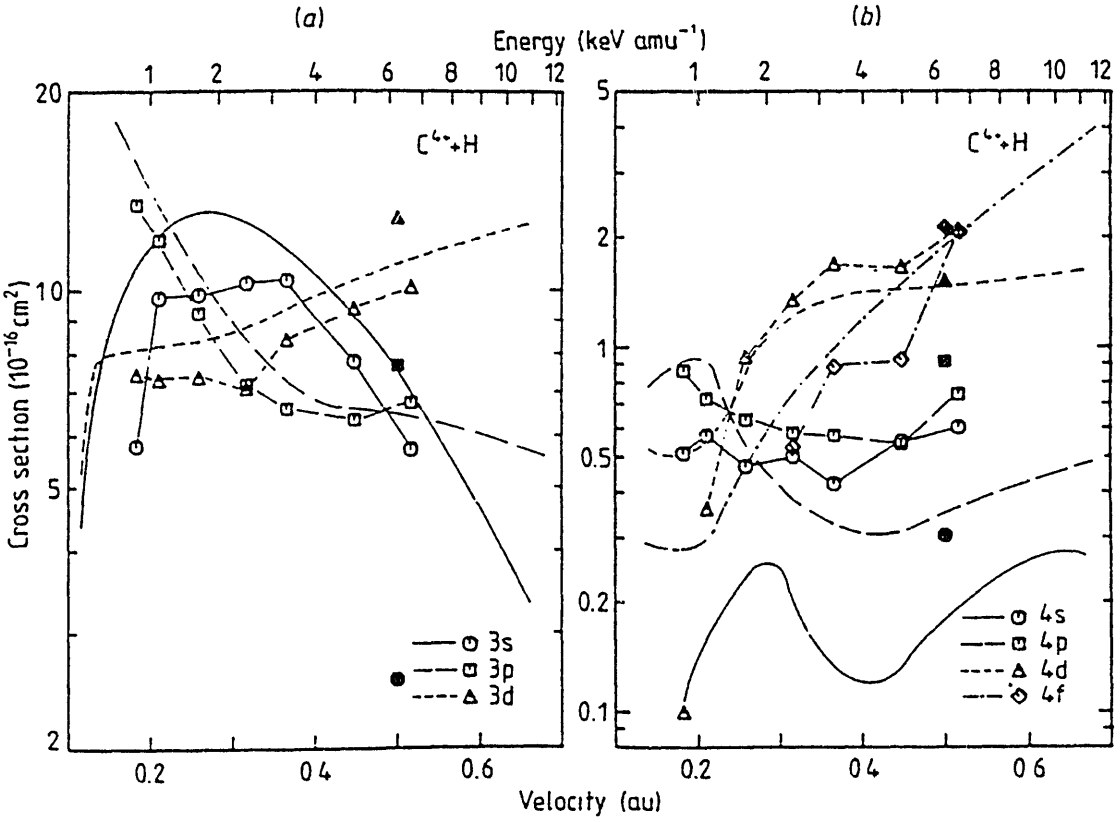

Fig.7a Comparison of theoretical and experimental cross sections for electron capture into 3l and 4l states of C^{3+} ions in C^{4+} + H collisions[12].

Observations in Ne^{q+}(q=1-10) + Na ($n_0 \cong 10$) collisions at relatively low energies ($\cong$250 eV/amu) suggest that an electron is captured mostly into lower l-states

(which result in X-ray emission) as the cross sections for visible lines (which result from transitions between higher l-states) are only 1/30 of total electron capture cross sections[14].

3.3 m-distributions

For bare ion + H(1s) collisions, rotational mixing among m-states occurs at our energy range, with the final m-substate distributions of varied degree of alignment[15] :

a) at low velocities ($v_i << v_e$), m=0.

b) at intermediate velocities (finite rotational velocities), some rotational mixing among m-substates occurs with high degree of alignment, m=0,$\pm$1 (not statistical).

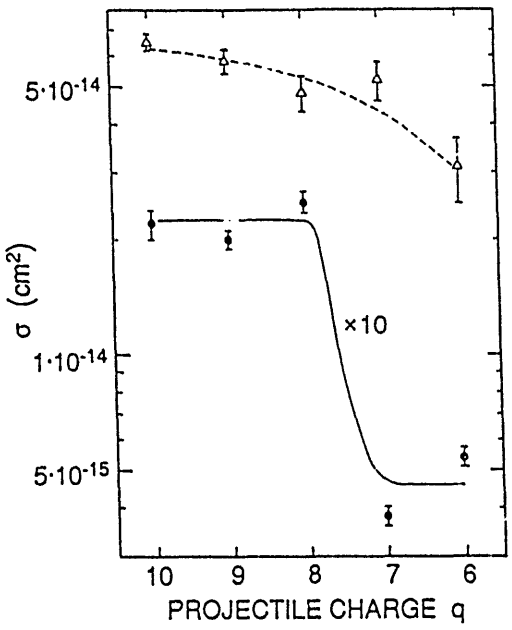

Fig.7b Comparison of cross sections of visible photon emissions (solid line) to total electron capture cross sections (dotted line)[14].

However, polarization measurements to determine m-distributions are still very limited (only for p states).

In Ne^{q+} + Na collisions, experimental values of polarization for $-n = -1$ (for example n=10->n=9 for q=10) seem to be in agreement with the calculated m-

distributions for q=10-8, meanwhile those for q≤7 are much smaller than calculation, suggesting that the estimated m-distributions are much wider than calculation due to core electron effect[14] (see Fig. 7c).

For multiple electron transfer, the influence due to multiple-electron stripped residual ions should become larger than that in single electron capture. This remains to be confirmed.

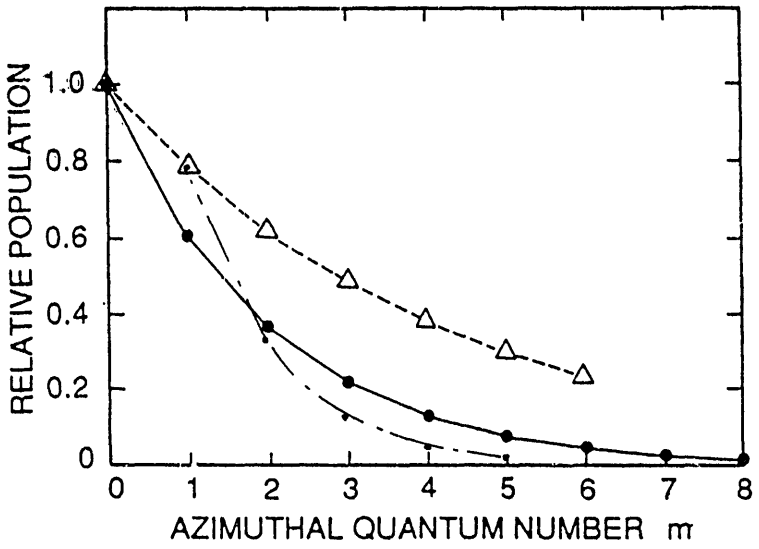

Fig. 7c Estimated m-distributions in Ne^{q+} + Na collisions. The solid line is for q=9 and the dashed line is for q=6[14]. The dash-dotted line is the calculated value for Ne^{10+} + H collisions[15].

3.4 Autoionization states

A number of doubly or multiply excited states formed through electron capture can be autoionized whose important information can be obtained through analysis of the emitted electron spectra. For example, autoionizing electron spectra in N^{7+} + He -> Ne^{5+}(3131') + He^{2+} collisions reveal that electrons are dominantly captured (≅ 50 %) into highest l-state $^2G(2,0)$(which means that two electrons captured sit on the opposite sides of nucleus)[16](see Fig.7d). The detailed analysis of electron spectra in some cases indicates that radiative cascades are negligibly small, suggesting that observed electron spectra reflect the

initial electron capture itself. **Some electron spectroscopic work should be also made for multi electron (>3) capture processes.**

On the other hand, as the autoionizing states emit electrons, then, the final product such as N^{6+} from $N^{5+}(31,31')$ state can also be studied with translational energy spectroscopy, though its energy resolution is limited. However, as the product of multiple electron capture processes is scattered into large angles, their angular distributions have to be known (see 4 and 5).

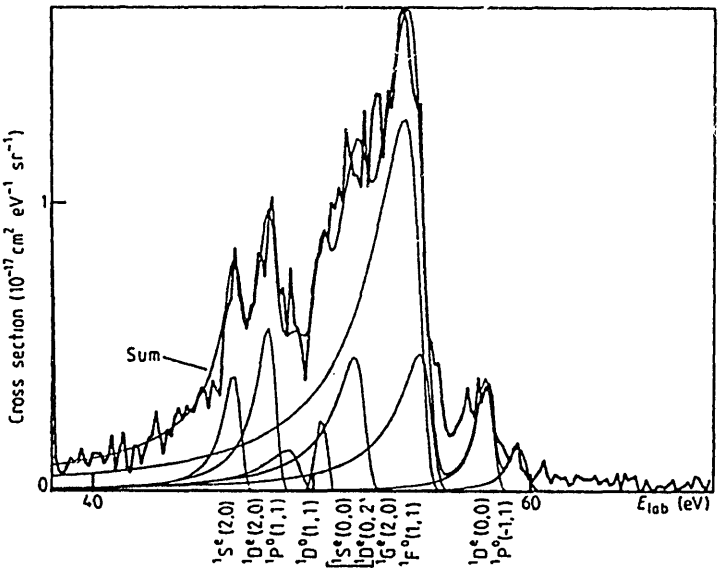

Fig. 7d Electron spectrum from autoionization of $Ne^{5+}(n,n')$ in Ne^{7+} + He collisions[16].

4. Angle-differential cross sections

Only few cases have been studied for their angular distributions. In C^{4+} + He -> C^{2+} + He^{2+} system, Steuckelberg oscillations have been observed experimentally and confirmed theoretically[17]. In most of multiple electron capture processes, projectile ions are scattered into larger angles, compared with single electron capture, because of strong Coulomb repulsion between collision partners after collisions[18] (see Fig. 8a).

Angular distributions of charge-selected projectiles in coincidence with charge-selected recoil ions can provide much detailed information of ion-atom

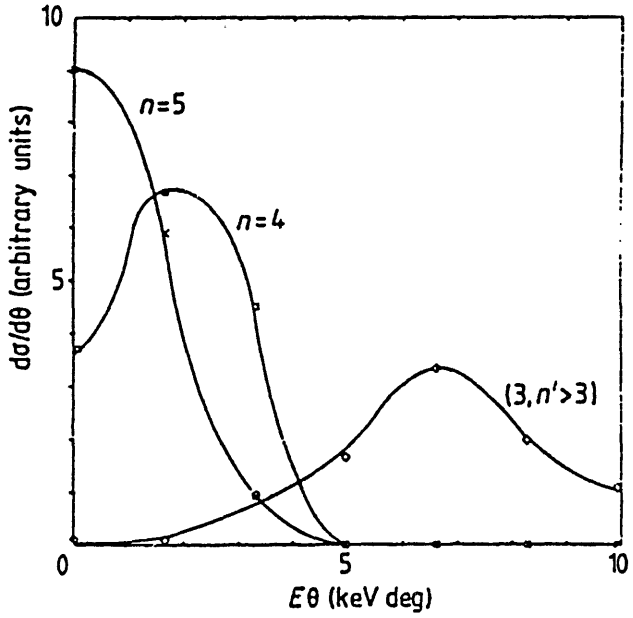

Fig. 8a Angular scattering cross sections for 16 keV Ne^{9+} + He collisions[18].

collisions[19]. Single electron capture process at 90 keV Ne^{7+} + Ne collisions is found to be strongly forward-peaked, indicating the dominance of soft collision with large impact parameters. With increasing the number of the captured electrons, large angle scattering becomes important(see Fig.8b). In multiple electron capture processes, autoionization of the captured ions play a role, resulting in the enhancement of ionic charge with increasing the number of captured electrons. Indeed, for recoil Ne^{6+} ion production, single and double autoionization processes are found to become dominant but no 6-electron transfer into ions resulting in projectile Ne^{+} can be observed. The measured charge distributions are also found to be sharper than that expected from binomial distributions and shifted toward higher charge, suggesting significant autoionization in collision partners.

At large-angle scatterings (>10 mrad), the mean charge of projectile and recoil ions are nearly the same, indicating that both particles form a quasimolecule and share equally the remaining electrons (in L-shell) (see Fig. 8c). The correlation diagram is of great help for understanding the processes.

Finally, in determining total cross sections for multi-electron capture, such angular distributions have to be known accurately (see 2).

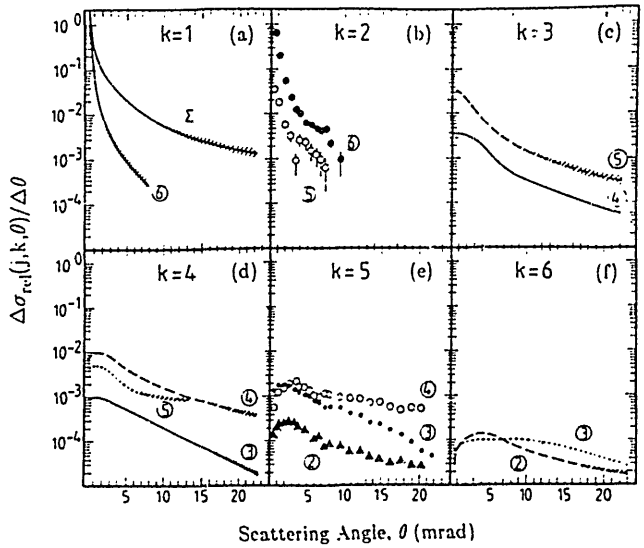

Fig. 8b Angular scattering for 90 keV Ne^{7+} + Ne -> Ne^{j+} + Ne^{k+} collisions. The projectile charge j is indicated with circles[19].

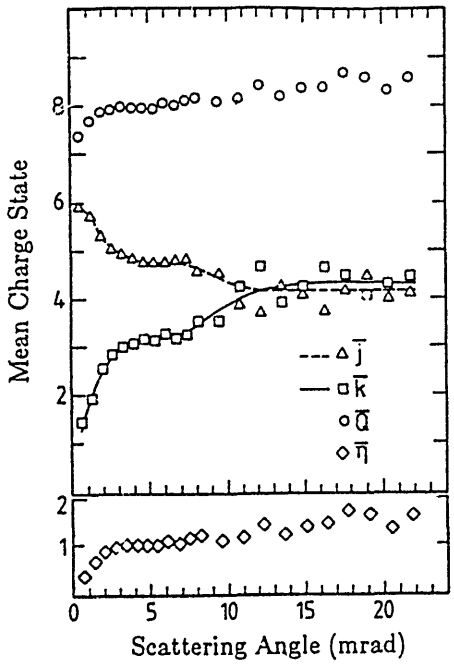

Fig. 8c Mean charges of projectile and recoil ions in 90 keV Ne^{7+} + Ne collisions as a function of the scattering angle[19]. Q and ñ are the mean total charge and the mean number of electrons emitted by autoionization.

References to III

1. R.K.Janev, L.P.Presnyakov & V.P.Shevelko, Physics of Highly Charged Ions (Springer, 1985)
2. H.Ryufuku, K.Sasaki & T.Watanabe, Phys. Rev. A 21 (1980) 745
3. A.Salop & R.E.Olson, Phys. Rev. A 13 (1976) 1312
4. K.Taubjerg, J. Phys. B 19 (1986) L367
5. A.Muller & E.Salzborn, Phys. Letters 62A (1977) 391 ; E.Salzborn & A. Muller, Electronic and Atomic Collisions (North-Holland, 1980) p.407
6. J.W.Gallagher, B.H.Bransden & R.K.Janev, J. Phys. Chem. Ref. Data 12 (1983) 873 ; H.Tawara, T.Kato & Y.Nakai, At. Data & Nucl. Data Tables 32 (1985) 235 ; W.K.Wu, B.A.Huber & K.Wiesemann, At. Data and Nucl. Data Tables 40 (1988) 57

6a. T.Iwai, Y.Kaneko, M.Kimura, N.Kobayashi, S.Ohtani, K.Okuno, S.Takagi, H.Tawara & S.Tsurubuchi, Phys. Rev. A 26 (1982) 105

7. H.Tawara, T.Iwai, Y.Kaneko, M.Kimura, N.Kobayashi, S.Ohtani, K.Okuno, S.Takagi & S.Tsurubuchi, J. Phys. B 18 (1985) 337

7a. M.Gargaud & M.McCarroll, J. Phys. B 21 (1988) 513

8. L.Liljeby, G.Astner, A.Barany, H.Cederquist, H.Danared, S.Huldt, P.Hvelplund, A.Johnson, H.Knudsen & K.G.Rensfelt, Phys. Scripta 33 (1986) 310 ; D.H.Crandall, Phys. Rev. A 16 (1977) 958
9. W.Groh, A.Muller, C.Achenbach, A.S.Schlachter & E.Salzborn, Phys. Letters 85A (1981) 77
10. H.Y.Wang & D.A.Church, Phys. Rev. A 36 (1987) 4261

10a. K.Dolder & B.Peart, Rep. Prog. Phys. 48 (1985) 1283

11. C.Harel & H.Jouin, J. Phys. B 21 (1988) 859
12. D.Dijkkamp, D.Ciric, E.Vlieg, A.de Boer & F.J.de Heer, J. Phys. B 18 (1985) 4763 ; R.Hoekstra, D.Ciric, A.N.Zinoviev, Yu.S.Gordeev, F.J.de Heer & R.Morgenstern, Z. Phys. D 8 (1988) 57

13. W.Fritsch & C.D.Lin, J. Phys. B 17 (1984) 3271

14. L.J.Lembo, K.Danzmann, Ch.Stoller, W.E.Meyerhof & T.W.Hansch, Phys. Rev. A 37 (1988) 1141

15. A.Salin, J. de Phys. 45 (1984) 671

16. A.Bordenave-Montesquieu, P.Brenoit-Cattin, M.Boudjema, A.Gleizes & H.Bachaus, J. Phys. B 20 (1987) L695 ; S.Tsurubuchi, T.Iwai, Y.Kaneko, M.Kimura, N.Kobayashi, S.Ohtani, K.Okuno, S.Takagi & H.Tawara, J. Phys. B 15 (1982) L733

17. H.Danared, H.Andersson, G.Astner, A.Barany, P.Defrance & S.Rachafi, J. Phys. B 20 (1987) L165 ; Phys. Scripta 36 (1987) 756 : L.N.Tunnell, C.L.Cocke, J.P.Giese, E.Y.Kamber, S.L.Varghese & W.Waggoner, Phys. Rev. A 35 (1987) 3299

18. M.Barat, M.N.Gaboriaud, L.Guillemot, P.Roncin, H.Laurent & S.Andriamonje, J. Phys. B 20 (1987) 5771

19. H.Schmidt-Bocking, M.H.Prior, R.Dorner, H.Berg, J.O.K.Pedersen, C.L.Cocke, M.Stockli & A.S.Schlachter, Phys. Rev. A 37 (1988) 4640

IV. Collisions with solid surfaces at low energies

1. Scattered particles from surface

The scattering processes of projectile ions from surfaces and their mechanisms are dependent on three phases[1] :

a) soft collisions with near-surface atom in the incoming path

b) violent collisions with solid target atom

c) soft collisions with near-surface atom in the outgoing path.

Here electron transfer processes in collisions with surfaces play an important role in determining the fractions of neutral and charged particles. The main electron transfer processes of ions in collisions with solids are as follows (see Fig.1)[2] :

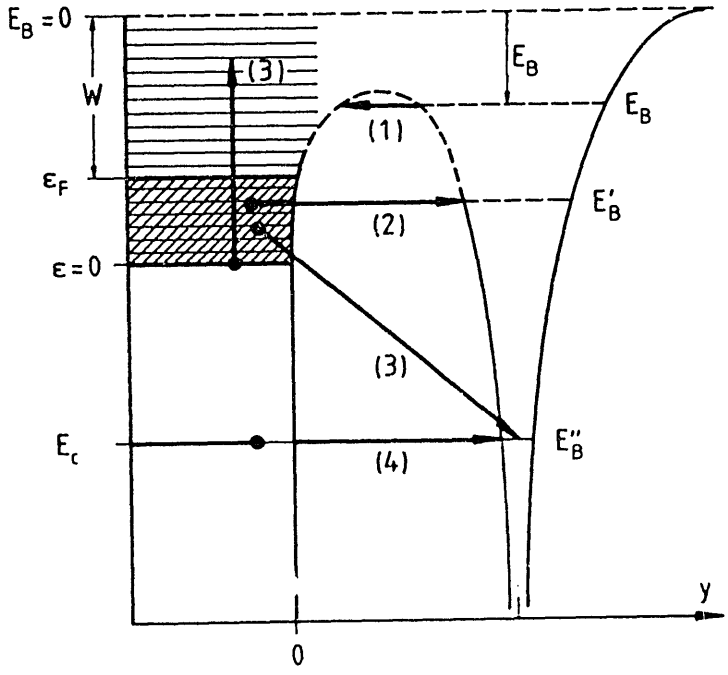

Fig.1 Some important electron transfer processes in collisions with solids[2].

1) resonant electron transfer between metal valence band and a discrete projectile state (projectile resonant ionization)

2) resonant electron transfer into a discrete projectile state (projectile neutralization)

3) Auger (or radiative) transition involving metallic continuum states and a

discrete projectile state

4) transition between a discrete (innershell) state of metal and a discrete projectile state.

Although details are dependent upon a number of parameters such as the incident angle or the incident ionic charge, the observed data suggest that scattered particles are mostly neutral and a very small fraction of singly and doubly charged ions are included in the scattered particles. Only a far small fraction of trebly charged ions are seen even in relatively high charge ion incidence.

1.1 Charge distribution and electronic states of scattered particles

In Fig.2a are shown the fractions of Ne, Ar and Kr ions taken at 15° under 20 keV impact on clean tungsten surface at 15° incidence. From these figures, the followings can be summarized[3] :

a) the fraction of singly charged ions in the scattered ions is nearly independent of the incident ionic charge,

b) this can be understood from the fact that the ionic state of ions after a series of collisions with surface atoms is determined through successive Auger neutralization and deexcitation processes. The time for these processes is of the order of 10^{-15} s which is the same order of magnitude as the time that the incident ions spend near or on surface,

c) the fraction of doubly charged ions is sharply increased at Ne^{9+}, Ar^{9+} and Kr^{9+} incidence and that of trebly charged ions is much drastically enhanced. Note that they carry a single vacancy in K-, L- and M-shells, respectively,

d) this is because the time requiring to fill the innershell vacancies is much longer than that for low charge ions. Thus, even after violent collisions, some fraction of highly charged incident ions can survive throughout collisions with surface. The resulting scattered projectiles should be in highly excited states and when they leave the surface, they

can decay by autoionization, resulting in the increase of the ion charge. For example, a significant part of trebly charged ions are due to doubly charged ions which are autoionized on the outgoing channel,

e) Further information can be obtained through observation of their energy after scattering : the energy distributions of the doubly and trebly charged scattered particles have no low energy tails, meanwhile those of singly charged ions have a large portion of low energy tails (see Fig. 2b). This is particularly significant in higher charged ion incidence. This fact suggests that the low energy tails result from a series of collisions of the incident ions with target atoms in solids,

f) However, no experimental work has been reported on the electronic states of the scattered particles. Under some conditions, the projectile ions have innershell vacancies as observed through Auger electrons or X-ray spectra (see 2.4).

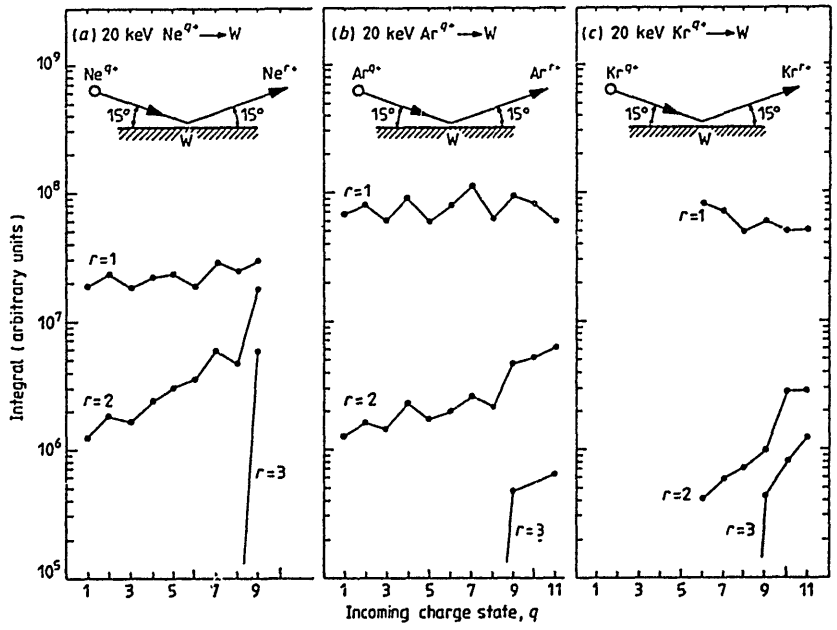

Fig. 2a Yields of scattered Ne, Ar and Kr ions with the charge of r=1, 2 and 3 in the incidence charge q = 1-11 on tungsten surface[2].

It is important to know their electronic state of scattered ions, in particular of singly or doubly charged ions when ions with very high charge collide with

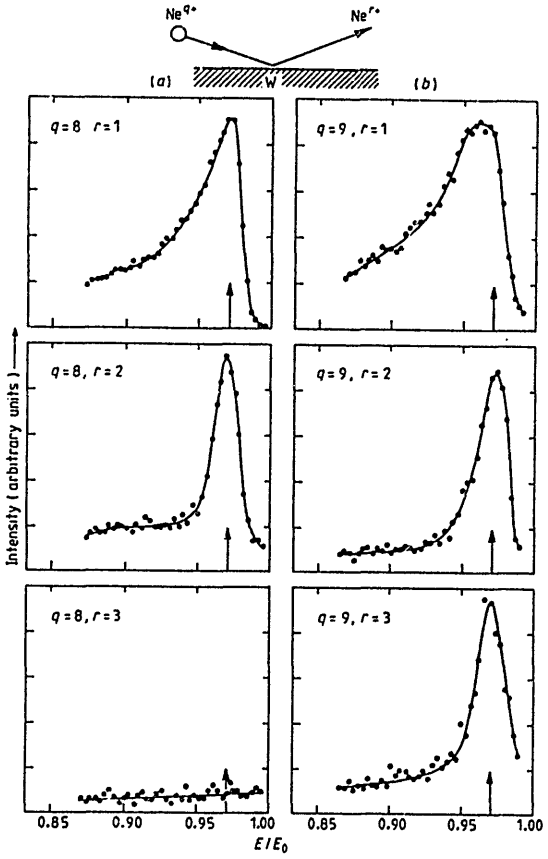

Fig. 2b Energy distributions of scattered Ne ions from pure tungsten surface. q and r indicate the charge of the incident and scattered particles[3]. Note that energy broadening toward lower energy is significant for singly charged scattered ions.

1.2 Zero-angle or grazing incidence collision processes

It is expected that a series of new phenomena can occur under such extreme collision conditions (theta≅0)[4]. In fact, the grazing incidence can provide unique technique to investigate collision processes of highly charged ions with surface[2]. In such grazing incidence conditions, the projectile ion energy parallel to surface is almost the same as their initial energy (E_0) : $E_x \cong E_0$, meanwhile that normal to the surface is roughly given as $E_y=E_0*\sin^2(\text{theta})$. For

theta≅0.2', $E_y/E_x \cong 10^{-5}$. This means that we can study collision processes of highly charged ions with extremely small energy with surface using ions with relatively high energy which can be easily handled and focused under the well controlled conditions.

From a series of measurements[5], the charge distributions of the scattered ions after grazing incidence have been found to be quite different from those after passing foils. Such difference is strongly dependent on the combination of ion-surface atom and can be qualitatively understood from dynamic variation of their potential energy as a function of the distance between the incident ion and surface (due to image potential of the ion inside solid).

For Li^+ + Cu system, the outershell electron (2s) of Li projectile ions can be easily resonant-ionized through electron transfer into empty states above the Fermi level of Cu (process (1) in Fig.1).

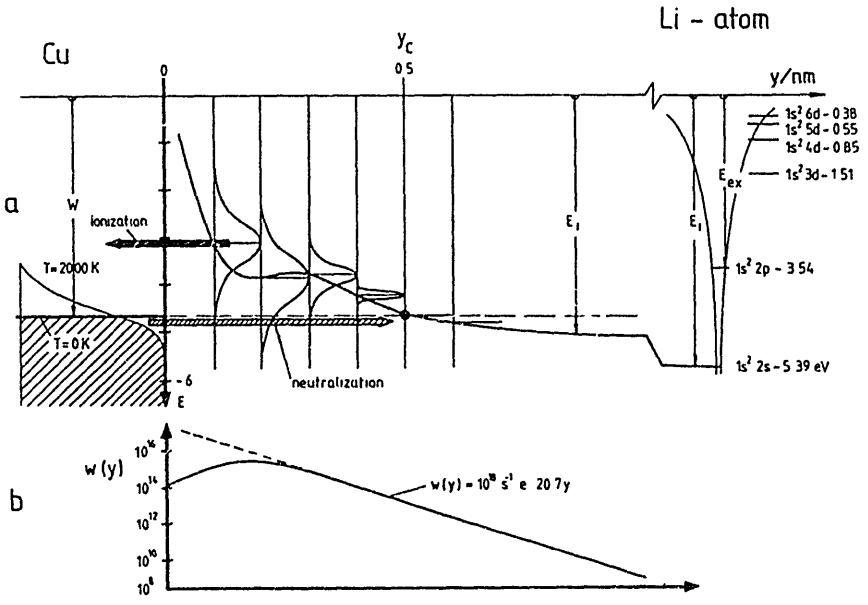

Fig.3 Variation of the potential energy as a function of the nuclear distance in Li^+ + Cu collisions[2].

Furthermore, as seen in their energy curve (see Fig.3), with the ions approaching surface, the potential energy level of 2s electron of Li ions

goes over the Fermi level of Cu target. Then, the resonant-ionization probabilities of Li 2s electron are enhanced. Therefore, the fraction of neutral beams decreases significantly, compared with those from foils. On the contrary, for N^+ + Cu system, the situation becomes reverse, namely the resonant-electron capture (process (2) in Fig.1) is dominant. Thus, the fraction of neutral component of N ions is enhanced.

Until now, no investigation on grazing incidence of highly charged ions has been performed at lower energies.

2. Emitted electrons

2.1 Total electron emission g

Total electron emission g defined as ratio of the emitted secondary electrons per incident ion, is believed to consist of two components[6] (see Fig.4):

$$g = g(PE) + g(KE),$$

where g(PE) is the term due to the potential emission and g(KE) is due to the kinetic emission.

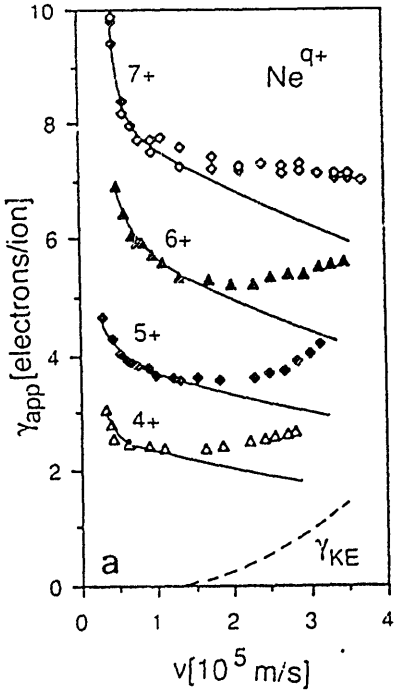

Fig. 4 Secondary electron emissions from solid surfaces as a function of the collision velocity of Ne^{q+} (q=4-7) ions on clean Au surface[6].

The first potential emission term, g(PE), has the following features[7] :

a) the electron emission is due to interactions of vacant states of projectiles with surface valence-band states,

b) as no kinetic energy of projectiles is necessary, it is dominant at low energies (< $1*10^7$ cm/s) and decreases with increasing the collision energy (due to the decreasing time for resonance neutralization and autoionization, followed by slow electron emission),

c) at low velocities, g(PE)=k*W where W is total potential energy available from the incident ions equal to the sum($I_{i-1,i}$), $I_{i-1,i}$ being ionization potential from i-1 to i ionic states,

d) g(PE) is roughly independent of ionic charge but dependent on their ionization potential energy W, e) roughly 100 eV of the energy is required for a single electron emission due to potential emission mechanism.

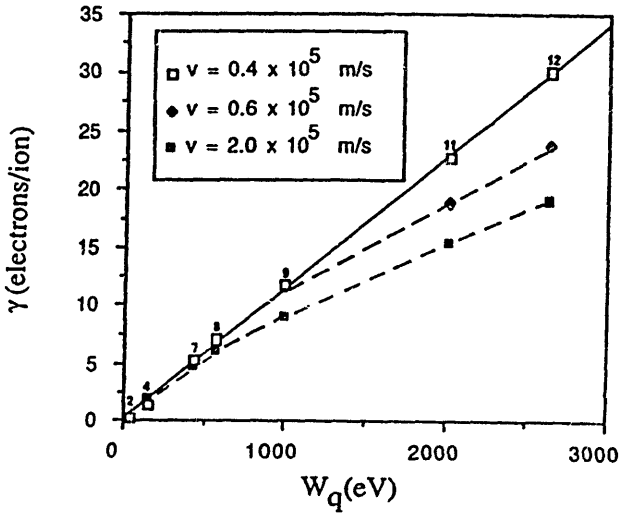

Fig. 5 Dependence of total electron emission yield from clear Au surface on potential energy of the incident Ar^{q+} (q=2-12) ions at various collision velocities[8].

On the other hand, the kinetic emission term g(KE) has the following features :

a) electron emission occurs through close collisions between projectile and target atom and thus need some minimum kinetic energy which roughly

corresponds to about $1*10^7$ cm/s and increases with the collision energy and finally becomes dominant over the potential emission at higher energies,

b) the emission rate is independent of the ionic charge[8] but dependent only on W.

The above relation is valid only at low energies ($<1*10^7$ cm/s), meanwhile, at higher energies and also for higher charge ions, g levels off at higher W. This is due to the increased time necessary for successive neutralization for higher charge ions. Then only partial neutralization can occur before highly charged ions hit the surface (see Fig. 5).

The neutralization time for multiply charged ions at lower energies can be estimated as follows :

the number of collisions for complete neutralization is given as

$$N=W/W_0$$

where W is total potential energy available from projectiles and W_0 is the average energy required for neutralization($\cong$15 eV). Thus, the complete neutralization time is N*t where t is the average time for a single resonant capture + Auger decay ($\cong 10^{-15}$ s). On the other hand, the electron capturing state n_c for hydrogenic ions can be given as $E_n = (1/2)(q/n_c)^2$, and the electron classical orbital radius for this state, $r = n_c^2 a_0/q$, the distance occurring resonance electron transfer is assumed to be a few times of the electron orbital radius, $d\cong 5*r$ and the time of passage of ions is estimated to be d/v, with the ion velocity v.

Thus, roughly speaking, at the velocities below 10^7 cm/s, complete neutralization can be achieved for most of intermediate charge ions as follows : For Ar^{12+} ions with the potential energy=2650 eV, N=177 and, then, the total neutralization time is $177*10^{-15}\cong 1.8*10^{-13}$ s. On the other hand, n_c=20, r=18 A, and then d=100 A. Thus, the transit time is about 10^{-13} s (for velocity of 10^7

cm/s). However, for very heavy ions such as U^{92+} ions, even the velocity of 10^6 cm/s seems to be too large for complete neutralization (total potential energy=740 keV : time for complete neutralization = $5*10^{-11}$ s : time of passage = $6*10^{-12}$ s). In this case, only 10 % of the incident beams can be neutralized before they hit the target surface and, thus, they should still have a plenty of the innershell vacancies at the time they arrive at the surface (here we should take into account very strong image effect for more precise discussion[2] and thus the transit time become small, indicating much less incomplete neutralization). The following topics have to be investigated for further understanding of neutralization : **how large is g(PE) for very high charge ions with PE >> KE, in particular at the lowest energies ?** and **how does g(PE) depend on the incident angle to surface, in particular at grazing incidence ?**
The angular distributions of the emitted electrons (number, energy, etc.) have also to be determined.

2.2 The number of emitted electrons

In addition to the above parameter concerning with secondary electron emission from surface, the real number of emitted electrons per incident ion is also an important parameter to get information on collision processes. Such measurements had already been made some time ago for use of zero-time detection of ions passing through thin foils which were kept at high voltage of 20 - 30 keV. The number of electrons emitted from solid can be known from the collected charge, for example, on a surface-barrier detector. Because of the limitation of its energy resolution, up to 12 electrons could be resolved in passage of 2 - 5 MeV alpha particles(see Fig.6).

At our situation of relatively low energies, the solid must be at the ground potential, meanwhile the detector is at high voltage. This accompanies serious noises. In low energy Ar^{12+} ion impact, about 30 electrons are estimated to be emitted (see Fig. 5). With the Poisson distribution, it is expected that a

considerable fraction of ions emit as much as 60 electrons, which need some elaborate techniques to be resolved.

2.3 electron energy distribution

In contrast to the ratios of electron emission to the incident ion, the energy distributions of emitted electrons have much information to understand collision mechanisms in highly charged ion collisions with solids. In an experiment by Delaunay et al. using 15-70 keV Ar^{9+} ions normal incident upon Au[10], the following features have been reported (see Fig.7):

a) the mean energy is around 6 eV (roughly independent of projectile energy), b) the width (FWHM) is about 15 eV, c) these parameters are weakly dependent on the velocity but increase with increasing the ionic charge, d) in the case $g \cong W$, the mean energy, peak position and width are roughly constant, e) in the case $g \neq W$, the peak becomes broad for higher charge ions, suggesting the variation of the ionic states during electron emission.

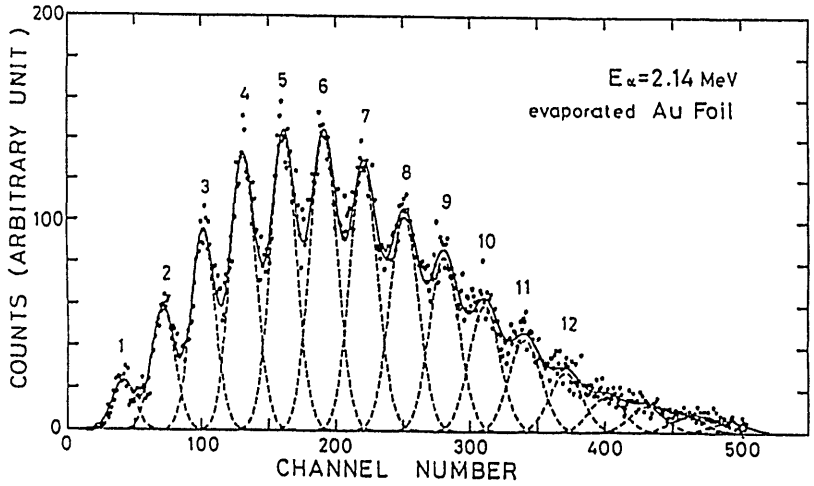

Fig. 6 Distribution of the number of emitted electrons in passing 2.4 MeV alpha particles through evapolated gold foils[9].

2.4 Auger electrons

Although weak (only a few %), compared with low energy electrons described above, they contain important information on innershell electron processes which might be involved in ion collisions with solids[10,11] (see Fig. 8) :

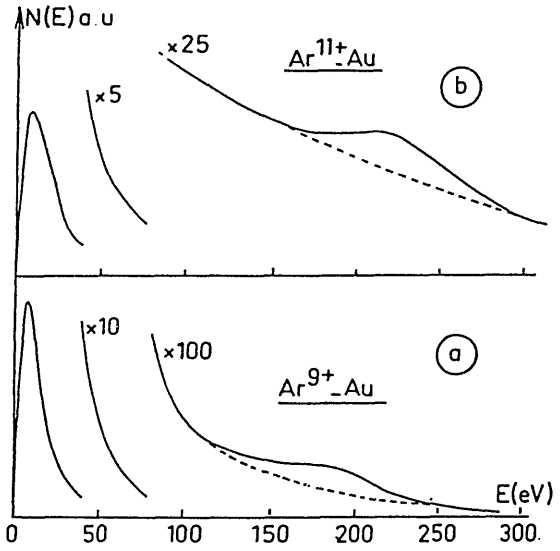

Fig. 7 Energy distributions of electrons emitted from Au in Ar^{9+} and Ar^{11+} ions incident upon clear Au surface[10].

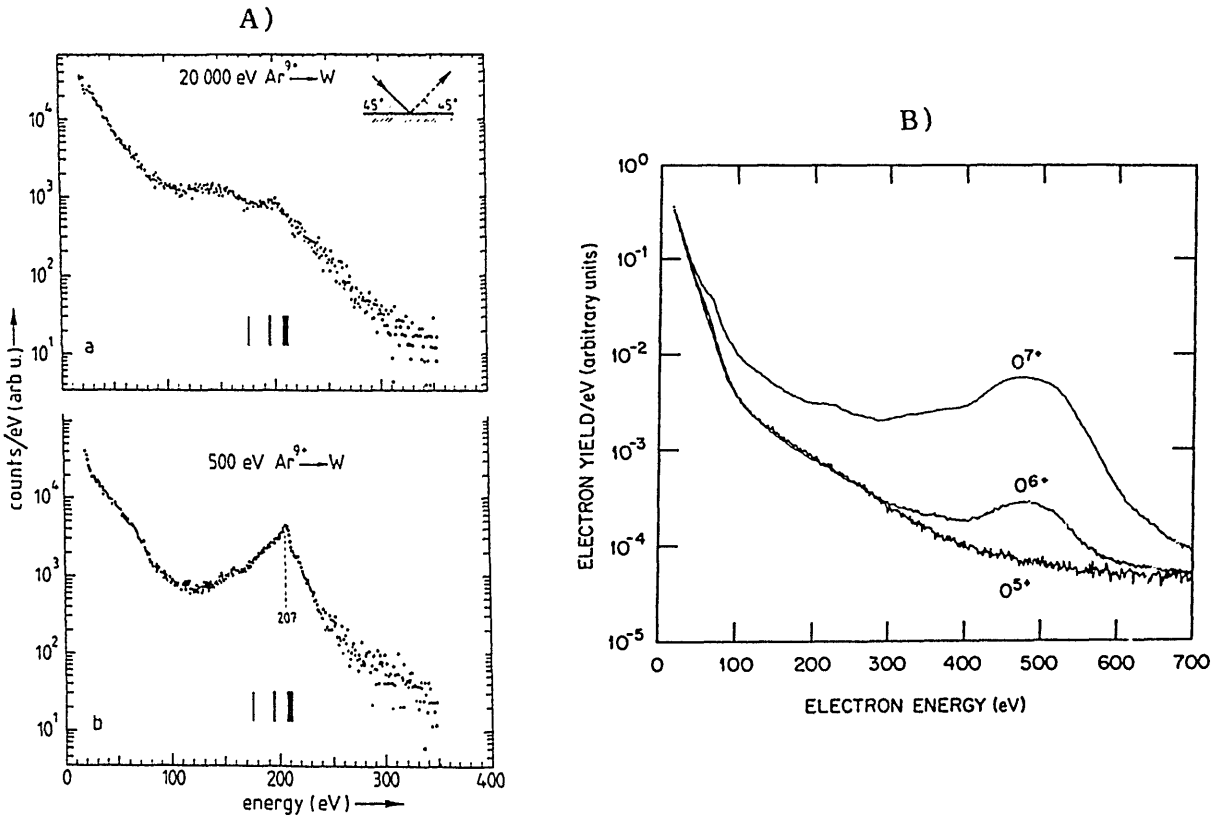

Fig. 8 Auger electron spectra from solids by highly charged ion impact.

A) 500 eV and 20 keV Ar^{9+} ions on tungsten surface[11].

B) 60 keV O^{q+} (q=5,6,7) ions on Au(110) surface[12].

a) LMM Auger electrons of Ar ions from Ar^{q+}(q<8) + Au collisions are very weak,

b) the Auger electron emissions become significant if the incident ions have innershell (L-) vacancies. For example, 500 eV Ar^{9+} ions with a single 2p vacancy produce significant $L_{23}MM$ Auger electron peaks at around 120-240 eV which is found to be very much different from the expected value from direct Auger neutralization to Ar^{9+} ions (450 eV : no peak is seen there) but very similar to that from neutral Ar atom targets or Ar^{+} + solid collisions,

c) this fact suggests that, prior to Auger decay, the outer M-shell vacancies are already filled while the L-shell vacancies are still alive at low velocities. Thus, LMM Auger electrons are sharp and Doppler-shifted, indicating that the decay of innershell vacancies occurs before ions hit the surface,

d) with increasing the collision energy, Auger electron yields from Ar^{9+} collisions decrease due to decrease of the time near the surface and thus ions reach the surface before deexcitation occurs (note those for Ar^{+} collisions increase with increasing the collision energy due to binary collision),

e) for somewhat higher charge Ar^{11+} collisions, Auger peak at 150-300 eV is energy-shifted due to some still-survived 2p vacancies because of the longer neutralization times for higher charged ions,

f) at higher energies, ions with L-shell vacancies penetrate into solid before complete neutralization could be achieved. Inside solid, the outershell electrons of ions are stripped off or screened by metal electrons. Thus the level structures should change and the electron energy spectrum also changes (in fact, for 20 keV Ar^{9+} ion collisions, another small peak around 150 eV is seen),

g) for O^{7+} ions with K-shell vacancies, KLL Auger spectra with similar features have been observed[12] (see Fig. 8),

h) **X-ray spectroscopy might also provide information on the electronic states of ions before/during/after collisions.**

3. Sputtering

It has been known[13] sometime that sputtering of atoms from solis by ion impact is due to kinetic collision cascades. Thus, the sputtering yield, defined as ratio of sputtered particles to the incident particle, should not strongly depend on the electronic or ionic state of the incident particles. On the other hand, experimental observations of Arifov et al.[14] and Radzhabov et al.[15] show that sputtering yields from NaCl or ZnS increase with projectile ionic charge, meanwhile those from metals are independent of the ion charge over q=1-6. These investigations suggested that there was another mechanism for sputtering for non-metallic solids : electronic sputtering or Coulomb explosion[16] (See Fig. 9a).

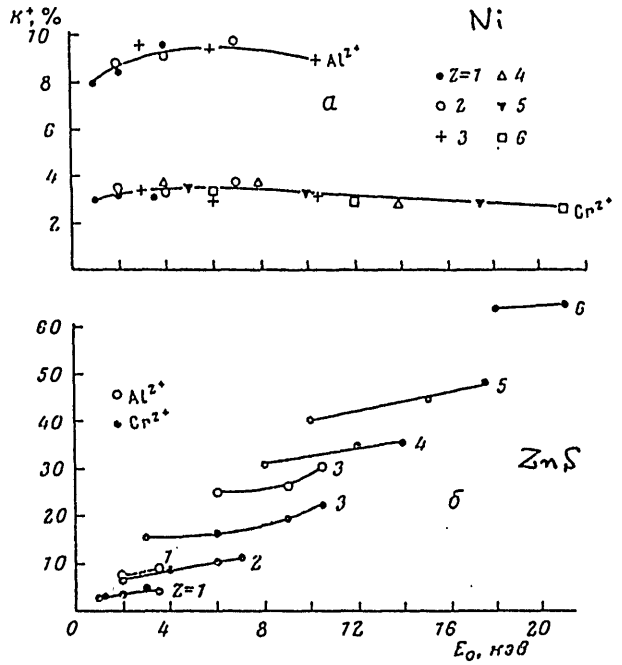

Fig. 9a Sputtering yields of metal (Ni) and non-metallic solid (ZnS) by ion impact[14]. The numbers beside curves indicates the ion charge state.

As there seemed some uncertainties in their work, particularly in surface characterization and some surface contamination might affect their measurements, recently de Zwart et al.[17] repeated similar measurements under much better surface conditions. Their sputtering yields in 20 keV Ar^{q+}(q=1-9) on Si in 6° incidence to surface normal reveal (see Fig.9b) :

a) yields of neutral Si atoms are roughly independent of the incident charge from q=1-9, with sputtering yield of 1.3 atoms/ion,

b) yields of secondary Si ions (supposed mostly singly charged) are constant over q=1-6 ($4x10^{-3}$ ions/ion, then starting to increase and reach $12x10^{-3}$ ions/ion for Ar^{9+} ions. These values are consistent with other measurements[18]. Note that Ar^{9+} ions have an L-shell vacancy.

c) this enhancement might be due to electronic sputtering ? However, sputtered Si ion yields from Ar^{9+} ion (total neutralization energy=1000 eV) are almost two orders of magnitude smaller than those from Al^{7+} ion (neutralization energy=759 eV) impact by Arifov et al., suggesting some surface effects in one of these measurements,

d) though this comparison could not give any finite answer to electronic sputtering because ion sputtering yields are a minor contribution to total sputtering, these results suggest the major features of sputtering by highly charged ions are practically the same as those by low charged ions,

e) this suggestion is also supported by the observation of very similar energy spectra of sputtered ions in both Ar^{+} and Ar^{9+} ion impact,[17]

f) **What happens in sputtering when the potential energy of projectiles becomes comparable to or larger than their kinetic energy ?**

To answer these questions, the following topics should be investigated :

#. detailed measurements of total (neutral and ion) sputtering yields.

#. energy distributions sputtered neutrals and ions.

#. their angular distributions

#. incidence angle dependence, in particular for grazing incidence.

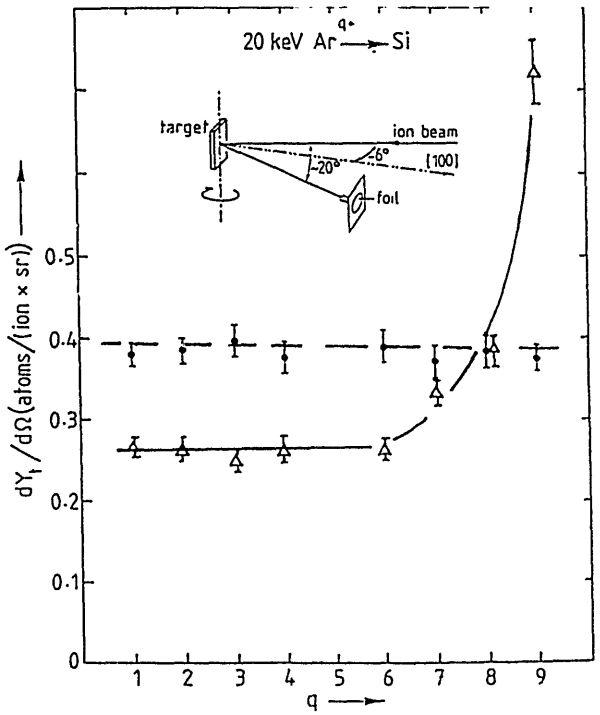

Fig. 9b Sputtered neutral (solid circle) and ion (open triangle) yields of Si target by 20 keV Ar^{q+} ion impact as a function of the ionic charge of projectiles q. Note that ion yields are multiply by a factor of 200.

References to IV

1. N.H.Tolk, J.C.Tully, W.Heiland & C.W.White (ed.), Inelastic Ion-Surface Collisions (Academic Press, 1977)
2. H.Winter and R.Zimny, Coherence in Atomic Collision Physics (Plenum, 1988) p.283
3. S.T.de Zwart, T.Fried, U.Jellen, A.L.Boers & A.G.Drentje, J. Phys. B 18 (1985) L623 ; K.J.Snowdon, Nucl. Instr. Meth. B 34 (1988) 309
4. J.Burgdorfer, E.Kupfer & H.Gabreil, Phys. Rev. A 35 (1987) 4963
5. H.Winter, R.Zimny, A.Schirmacher, B.Becker & H.J.Andra, Z. Phys. A 311 (1983) 267
6. M.Fehringer, M.Delaunay, R.Geller, P.Varga & H.Winter, Nucl. Instr. Meth. B 23 (1987) 245
7. M.Delaunay, M.Fehringer, R.Geller, D.Hitz, P.Varga & H.Winter, Phys. Rev. B 35 (1987) 4232
8. K.Oda, A.Ichimiya, Y.Yamada, T.Yasue & S.Ohtani, Nucl. Instr. Meth. B 33 (1988) 345
9. S.Mizugashira (private communication)
10. M.Delaunay, C.Benazeth, N.Benazeth, R.Geller & C.Mayoral, Surf. Sci. 195 (1988) 455
11. S.T.de Zwart, Nucl. Instr. Meth. B 23 (1987) 239
12. F.W.Meyer, C.C.Havener, K.J.Snowdon, S.H.Overbury, D.M.Zehner & W.Heiland, Phys. Rev. A 35 (1987) 317
13. R.Behrisch (ed.), Sputtering by Particle Bombardment 1 (Springer, 1981)
14. Y.Yu.Arifov, E.K.Vasileva, D.D.Gruich, S.F.Kovalenko & S.N.Morozov, Izv. Akad. Nauk SSSR, ser. Fiz. 40 (1976) 2621
15. Sh.S.Radzhabov, R.R.Rakhimov & D.Abdusalimov, Izv. Akad. Nauk SSSR, ser. Fiz. 40 (1976) 2543
16. I.S.Bitenskii, M.N.Murakhmetov & E.S.Parilis, Sov. Phys.-Tech. Phys. 24

(1979) 818

17. S.T.de Zwart, T.Fried, D.O.Boerma, R.Hoekstra, A.G.Drentje & A.L.Boers, Surf. Sci. 177 (1986) L939

18. K.Wittmaack, Sur. Sci. 90 (1979) 557

V. Concluding remarks

We have seen remarkable progresses on studies involving highly charged ions in collisions with electrons, atoms(ions) and solids. A great part of the success should owe to the development of powerful ion sources, such as EBIS and ECR. Although a number of the impressive work have been reported up to now, they are scattered and a lack of systematics. In particular, we are still short of information on the state-selected collision processes.

It is felt that we are almost ready for obtaining ions with much higher charge than before using EBIS and now we are surely at the stage of giving serious consideration in working with ultra-high charge ions such U^{92+} ions. There should be very interesting topics to be pursued experimentally as well as theoretically. What happens when very slow U^{92+} ions approach solids ? Because of very large total potential energy ($\cong$750 keV), complete neutralization of surfaces, in particular of non-metallic surfaces, can take too much time, before which a part of the surface may Coulomb-explode. It is also wondered if their electron capture processes could be understood just as an extension of our present knowledge, because their life times become so short that they may decay before the collision partners separate.

LIST OF IPPJ-AM REPORTS

IPPJ-AM-1* "Cross Sections for Charge Transfer of Hydrogen Beams in Gases and Vapors in the Energy Range 10 eV–10 keV"
H. Tawara (1977) [Published in Atomic Data and Nuclear Data Tables 22, 491 (1978)]

IPPJ-AM-2* "Ionization and Excitation of Ions by Electron Impact –Review of Empirical Formulae–"
T. Kato (1977)

IPPJ-AM-3 "Grotrian Diagrams of Highly Ionized Iron FeVIII-FeXXVI"
K. Mori, M. Otsuka and T. Kato (1977) [Published in Atomic Data and Nuclear Data Tables 23, 196 (1979)]

IPPJ-AM-4 "Atomic Processes in Hot Plasmas and X-Ray Emission"
T. Kato (1978)

IPPJ-AM-5* "Charge Transfer between a Proton and a Heavy Metal Atom"
S. Hiraide, Y. Kigoshi and M. Matsuzawa (1978)

IPPJ-AM-6* "Free-Free Transition in a Plasma –Review of Cross Sections and Spectra–"
T. Kato and H. Narumi (1978)

IPPJ-AM-7* "Bibliography on Electron Collisions with Atomic Positive Ions: 1940 Through 1977"
K. Takayanagi and T. Iwai (1978)

IPPJ-AM-8 "Semi-Empirical Cross Sections and Rate Coefficients for Excitation and Ionization by Electron Collision and Photoionization of Helium"
T. Fujimoto (1978)

IPPJ-AM-9 "Charge Changing Cross Sections for Heavy-Particle Collisions in the Energy Range from 0.1 eV to 10 MeV I. Incidence of He, Li, Be, B and Their Ions"
Kazuhiko Okuno (1978)

IPPJ-AM-10 "Charge Changing Cross Sections for Heavy-Particle Collisions in the Energy Range from 0.1 eV to 10 MeV II. Incidence of C, N, O and Their Ions"
Kazuhiko Okuno (1978)

IPPJ-AM-11 "Charge Changing Cross Sections for Heavy-Particle Collisions in the Energy Range from 0.1 eV to 10 MeV III. Incidence of F, Ne, Na and Their Ions"
Kazuhiko Okuno (1978)

IPPJ-AM-12* "Electron Impact Excitation of Positive Ions Calculated in the Coulomb-Born Approximation –A Data List and Comparative Survey–"
S. Nakazaki and T. Hashino (1979)

IPPJ-AM-13 "Atomic Processes in Fusion Plasmas – Proceedings of the Nagoya Seminar on Atomic Processes in Fusion Plasmas Sept. 5-7, 1979"
Ed. by Y. Itikawa and T. Kato (1979)

IPPJ-AM-14 "Energy Dependence of Sputtering Yields of Monatomic Solids"
N. Matsunami, Y. Yamamura, Y. Itikawa, N. Itoh, Y. Kazumata, S. Miyagawa, K. Morita and R. Shimizu (1980)

IPPJ-AM-15 "Cross Sections for Charge Transfer Collisions Involving Hydrogen Atoms"
Y. Kaneko, T. Arikawa, Y. Itikawa, T. Iwai, T. Kato, M. Matsuzawa, Y. Nakai, K. Okubo, H. Ryufuku, H. Tawara and T. Watanabe (1980)

IPPJ-AM-16 "Two-Centre Coulomb Phaseshifts and Radial Functions"
H. Nakamura and H. Takagi (1980)

IPPJ-AM-17 "Empirical Formulas for Ionization Cross Section of Atomic Ions for Electron Collisions –Critical Review with Compilation of Experimental Data–"
Y. Itikawa and T. Kato (1981)

IPPJ-AM-18 "Data on the Backscattering Coefficients of Light Ions from Solids"
T. Tabata, R. Ito, Y. Itikawa, N. Itoh and K. Morita (1981) [Published in Atomic Data and Nuclear Data Tables 28, 493 (1983)]

IPPJ-AM-19 "Recommended Values of Transport Cross Sections for Elastic Collision and Total Collision Cross Section for Electrons in Atomic and Molecular Gases"
M. Hayashi (1981)

IPPJ-AM-20 "Electron Capture and Loss Cross Sections for Collisions between Heavy Ions and Hydrogen Molecules"
Y. Kaneko, Y. Itikawa, T. Iwai, T. Kato, Y. Nakai, K. Okuno and H. Tawara (1981)

IPPJ-AM-21 "Surface Data for Fusion Devices – Proceedings of the U.S–Japan Workshop on Surface Data Review Dec. 14-18, 1981"
Ed. by N. Itoh and E.W. Thomas (1982)

IPPJ-AM-22 "Desorption and Related Phenomena Relevant to Fusion Devices"
Ed. by A. Koma (1982)

IPPJ-AM-23 "Dielectronic Recombination of Hydrogenic Ions"
T. Fujimoto, T. Kato and Y. Nakamura (1982)

IPPJ-AM-24 "Bibliography on Electron Collisions with Atomic Positive Ions: 1978 Through 1982 (Supplement to IPPJ-AM-7)"
Y. Itikawa (1982) [Published in Atomic Data and Nuclear Data Tables 31, 215 (1984)]

IPPJ-AM-25 "Bibliography on Ionization and Charge Transfer Processes in Ion-Ion Collision"
H. Tawara (1983)

IPPJ-AM-26 "Angular Dependence of Sputtering Yields of Monatomic Solids"
Y. Yamamura, Y. Itikawa and N. Itoh (1983)

IPPJ-AM-27 "Recommended Data on Excitation of Carbon and Oxygen Ions by Electron Collisions"
Y. Itikawa, S. Hara, T. Kato, S. Nakazaki, M.S. Pindzola and D.H. Crandall (1983) [Published in Atomic Data and Nuclear Data Tables 33, 149 (1985)]

IPPJ-AM-28 "Electron Capture and Loss Cross Sections for Collisions Between Heavy Ions and Hydrogen Molecules (Up-dated version of IPPJ-AM-20)
H. Tawara, T. Kato and Y. Nakai (1983) [Published in Atomic Data and Nuclear Data Tables 32, 235 (1985)]

IPPJ-AM-29 "Bibliography on Atomic Processes in Hot Dense Plasmas"
T. Kato, J. Hama, T. Kagawa, S. Karashima, N. Miyanaga, H. Tawara, N. Yamaguchi, K. Yamamoto and K. Yonei (1983)

IPPJ-AM-30 "Cross Sections for Charge Transfers of Highly Ionized Ions in Hydrogen Atoms (Up-dated version of IPPJ-AM-15)"
H. Tawara, T. Kato and Y. Nakai (1983) [Published in Atomic Data and Nuclear Data Tables 32, 235 (1985)]

IPPJ-AM-31 "Atomic Processes in Hot Dense Plasmas"
T. Kagawa, T. Kato, T. Watanabe and S. Karashima (1983)

IPPJ-AM-32 "Energy Dependence of the Yields of Ion-Induced Sputtering of Monatomic Solids"
N. Matsunami, Y. Yamamura, Y. Itikawa, N. Itoh, Y. Kazumata, S. Miyagawa, K. Morita, R. Shimizu and H. Tawara (1983) [Published in Atomic Data and Nuclear Data Tables 31, 1 (1984)]

IPPJ-AM-33 "Proceedings on Symposium on Atomic Collision Data for Diagnostics and Modelling of Fusion Plasmas, Aug. 29 – 30, 1983"
Ed. by H. Tawara (1983)

IPPJ-AM-34 "Dependence of the Backscattering Coefficients of Light Ions upon Angle of Incidence"
T. Tabata, R. Ito, Y. Itikawa, N. Itoh, K. Morita and H. Tawara (1984)

IPPJ-AM-35 "Proceedings of Workshop on Synergistic Effects in Surface Phenomena Related to Plasma-Wall Interactions, May 21 – 23, 1984"
Ed. by N. Itoh, K. Kamada and H. Tawara (1984) [Published in Radiation Effects 89, 1 (1985)]

IPPJ-AM-36 "Equilibrium Charge State Distributions of Ions ($Z_1 \geqq 4$) after Passage through Foils – Compilation of Data after 1972"
K. Shima, T. Mikumo and H. Tawara (1985) [Published in Atomic Data and Nuclear Data Tables 34, 357 (1986)]

IPPJ-AM-37 "Ionization Cross Sections of Atoms and Ions by Electron Impact"
H. Tawara, T. Kato and M. Ohnishi (1985) [Published in Atomic Data and Nuclear Data Tables 36, 167 (1987)]

IPPJ-AM-38 "Rate Coefficients for the Electron-Impact Excitations of C-like Ions"
Y. Itikawa (1985)

IPPJ-AM-39 "Proceedings of the Japan-U.S. Workshop on Impurity and Particle Control, Theory and Modeling, Mar. 12 – 16, 1984"
Ed. by T. Kawamura (1985)

IPPJ-AM-40 "Low-Energy Sputterings with the Monte Carlo Program ACAT"
Y. Yamamura and Y. Mizuno (1985)

IPPJ-AM-41 "Data on the Backscattering Coefficients of Light Ions from Solids (a Revision)"
R. Ito, T. Tabata, N. Itoh, K. Morita, T. Kato and H. Tawara (1985)

IPPJ-AM-42 "Stopping Power Theories for Charged Particles in Inertial Confinement Fusion Plasmas (Emphasis on Hot and Dense Matters)"
S. Karashima, T. Watanabe, T. Kato and H. Tawara (1985)

IPPJ-AM-43 "The Collected Papers of Nice Project/IPP, Nagoya"
Ed. by H. Tawara (1985)

IPPJ-AM-44 "Tokamak Plasma Modelling and Atomic Processes"
Ed. by T. Kawamura (1986)

IPPJ-AM-45 Bibliography of Electron Transfer in Ion-Atom Collisions
H. Tawara, N. Shimakura, N. Toshima and T. Watanabe (1986)

IPPJ-AM-46 "Atomic Data Involving Hydrogens Relevant to Edge Plasmas"
H. Tawara, Y. Itikawa, Y. Itoh, T. Kato, H. Nishimura, S. Ohtani, H. Takagi, K. Takayanagi and M. Yoshino (1986)

IPPJ-AM-47 "Resonance Effects in Electron-Ion Collisions"
Ed. by H. Tawara and G. H. Dunn (1986)

IPPJ-AM-48 "Dynamic Processes of Highly Charged Ions (Proceedings)"
Ed. by Y. Kanai and S. Ohtani (1986)

IPPJ-AM-49 "Wavelengths of K X-Rays of Iron Ions"
T. Kato, S. Morita and H. Tawara (1987)

IPPJ-AM-50 "Proceedings of the Japan-U.S. Workshop P-92 on Plasma Material Interaction/High Heat Flux Data Needs for the Next Step Ignition and Steady State Devices, Jan. 26 – 30, 1987"
Ed. by A. Miyahara and K. L. Wilson (1987)

IPPJ-AM-51 "High Heat Flux Experiments on C-C Composite Materials by Hydrogen Beam at the 10MW Neutral Beam Injection Test Stand of the IPP Nagoya"
H. Bolt, A. Miyahara, T. Kuroda, O. Kaneko, Y. Kubota, Y. Oka and K. Sakurai (1987)

IPPJ-AM-52 "Energy Dependence of Ion-Induced Sputtering Yields of Monatomic Solids in the Low Energy Region"
N. Matsunami, Y. Yamamura, N. Itoh, H. Tawara and T. Kawamura (1987)

IPPJ-AM-53 "Data Base on the High Heat Flux Behaviour of Metals and Carbon Materials for Plasma Facing Components – Experiments at the 10 MW Neutral Beam Injection Test Stand of the IPP Nagoya"
H. Bolt, C. D. Croessmann, A. Miyahara, T. Kuroda and Y. Oka (1987)

IPPJ-AM-54 "Final (n, ℓ) State-Resolved Electron Capture by Multiply Charged Ions from Neutral Atoms"
N. Shimakura, N. Toshima, T. Watanabe and H. Tawara (1987)

IPPJ-AM-55 "Atomic Data for Hydrogens in Collisions with Electrons – Addenda to IPPJ-AM-46"
H. Tawara, Y. Itikawa, H. Nishimura and M. Yoshino (1987)

IPPJ-AM-56 "Total and Partial Cross Sections for Electron Capture for C^{q+} (q= 6–2) and O^{q+} (q=8–2) Ions in Collisions with H, H_2 and He Atoms"
H. Tawara (1987)

IPPJ-AM-57 "Atomic Models for Hot Dense Plasmas"
K. Fujima (1988)

IPPJ-AM-58 "Recommended Data for Excitation Rate Coefficients of Helium Atoms and Helium-Like Ions by Electron Impact"
T. Kato and S. Nakazaki (1988)

IPPJ-AM-59 "Atomic and Molecular Processes in Edge Plasmas Including Hydrocarbon Molecules"
Ed. by H. Tawara (1988)

IPPJ-AM-60 "Theory of Threshold Energy of Ion-Induced Desorption by a Few-Collision Model"
Y. Yamamura, J. Bohdansky and E. Taglauer (1988)

IPPJ-AM-61 "The Application of Atomic and Molecular Physics in Fusion Plasma Diagnostics"
H. W. Drawin (1988)

IPPJ-AM-62 "Low Energy Atomic Collision Research Using Highly Charged Ions from EBIS and Other Ion Sources"
H. Tawara (1988)

Available upon request to Research Information Center, Institute of Plasma Physics, Nagoya University, Nagoya 464, Japan, except for the reports noted with*.